Mechanical properties Investigation of Composite material reinforced by uni-directional fibers

A Thesis

Submitted to the College of the Engineering / University of Kerbala in a Partial Fulfillment of Requirements for the Degree of Master of Science in Mechanical Engineering (Applied Mechanics).

Prepared by

Maytham Abd Alabas Oleiwi

(B.Sc. 2001)

Supervised By

Assist. Prof. Dr.   *Assist. Prof. Dr.*

Salah Noori Alnomani   *Mustafa Baqir Al-Khafaji*

2022   *1443هـ*

بسم الله الرحمن الرحيم

﴿ قَالُوا سُبْحَانَكَ لَا عِلْمَ لَنَا إِلَّا مَا عَلَّمْتَنَا إِنَّكَ أَنْتَ الْعَلِيمُ الْحَكِيمُ ﴾

صدق الله العلي العظيم

(البقرة: ٣٢)

Supervisors certification

We certify that this thesis entitled " *Mechanical properties Investigation of composite material reinforced by uni-direction fibers*" was   prepared by (*Mr.Maytham Abd Alabas Oleiwi*) and had been carried out completely under my supervision at the University of   Kerbala, Mechanical Engineering Department in partial fulfillment of the requirement for the degree of Master Science in Mechanical Engineering (Applied Mechanics).

Signature:

Supervisor: *Asst. Prof. Dr. Salah N. Alnomani*

Date: /   / 2022.

Signature:

Supervisor: *Asst. Prof. Dr. Mustafa B. Al-Khafaji*

Date: 6 / 4 / 2022.

Linguistic certification

I certify that the thesis entitled " *Mechanical properties Investigation of composite material reinforced by uni-direction fibers* " submitted by

"*Mr. Maytham Abd Alabas Oleiwi*" has been prepared under my linguistic supervision .Its language has been amended to meet the English style.

Signature:

Linguistic advisor: Asst. Prof. Dr. *Hayder Jabbar Kurji*

Date: / /2022

Examining Committee Certification

We certify that we have read this thesis entitled *"Mechanical properties Investigation of composite material reinforced by uni-direction fibers"* and as an examining committee, examined the student *"Maytham Abd Alabas Oleiwi"* in its content and what related to it, and that in our opinion it meets the standard of a thesis for the Degree of Master of Science in Mechanical Engineering (Applied Mechanics).

Signature:

Name: Asst. Prof. Dr. *Salah N. Alnomani*
(Supervisor)
Date: / /2022

Signature:

Name: Asst. Prof. Dr. *Ali Sabah Al-Turaihi*
(Member)
Date: 6 / 4 / 2022

Signature:

Name: Asst. Prof. Dr. *Mustafa B. Al-Khafaji*
(Supervisor)
Date: 6 / 4 / 2022

Signature:

Name: Dr. *Ahmed K. Hassan*
(Member)
Date: / /2022

Signature:

Name: Prof. Dr. *Farag Mahel Mohammed*
(Chairman)
Date: 1 / 4 / 2022

Approval of Mechanical Engineering Department

Signature:

Name: Asst. Prof. Dr. *Hayder Jabbar Kurji*
(Head of Mechanical Engineering Department)
Date: / /2022.

Approval of Deanery of College of Engineering / Kebala university

Signature:

Name: Prof. Dr. *Laith Shakir Rasheed*
(Dean of the College of Engineering)
Date: / /2022

<u>Dedication</u>

To My Mother & Father

To My wife and All My Family

To My Supervisors

To My All Friends

With Love and Respect

<u>Acknowledgements</u>

Abstract

In this work, the effect of fiber orientation and layers sequence on the properties will be studied Mechanical (strength, stiffness and fatigue) of carbon/epoxy composite material. The laminated composite materials were manufactured using Hand lay-up in vacuum technique with a volume fraction of 30%. This work consists of selecting the appropriate failure theory by comparing the experimental tensile test results of composite materials' lamina (carbon/epoxy) with different orientations (0° to 90°)with the five failure theories (Maximum stress theory, Maximum strain theory, Tsai-Hill theory, Tsai-Wu theory, and Ha shin's theory), a theoretical study of the effect of stacking sequence of layers with angles (0°,30°,60°,75° and 90°), on tensile strength using Hashin's theory, The laws of elasticity for composite materials and classical laminate theory to get the best sequence using the MATLAB program. The tensile test was performed for three sequences, where the sequence [60/30/0/90/75] represented the highest tensile value, the sequence [30/90/0/60/75] is represented the middle tensile value, and the sequence [0/30/60/90/75] is represented the minimum tensile value. The percentage difference between the theoretical and experimental tensile value results of the sequence [60/30/0/90/75] was 6.64%, while the percentage of the difference between the theoretical and experimental tensile value results of the sequence [30/90/0/60/75] was 9.34%. As for the sequence [0/30/60/90/75], the percentage of difference was 27%, and the fatigue properties of three stacking sequence laminated composite mentioned above have been measured experimentally under a constant stress ratio of R=-1 as a fully reversed bending load. The results showed that the sequence [60/30/0/90/75] that has the higher tensile strength had had better fatigue limits (60.08MPa and Nf > 106). Finally, the scanning electron microscope analysis (SEM) was used for investigating the morphology microstructure of the failed specimens of three sequence and mention above under the influence of fatigue

test, such as fibers breaking, matrix breaking, deboning between matrix and fiber, delamination, and transverse crack appearing, and that the failure shape were somewhat similar in all the sequences, but differed in the beginning of the damage from one layer to another due to the location of that layer in laminate, and its get away from center load.

Table of contents

Chapter four

Experimental work

Chapter five

Results and Discussion

List of Symbols

a. Alphabet Symbols

Symbol	*Description*	*unit*
$A_{c,f,m}$	*Area of cross-section of composite, fiber and Matrix respectively in model element.*	M^2
E_f	*Young's modulus of fiber.*	*GPa*
E_m	*Young's modulus of matrix.*	*GPa*
E_1	*Longitudinal young's modulus of composite Materials.*	*GPa*
E_2	*Transverse young's modulus of composite.*	*GPa*
$G_{f,m}$	*Shear modulus of fiber and matrix respectively.*	*GPa*
G_{12}	*Shear modulus in plane(1-2).*	*GPa*
M_f	*Mass fraction of fiber.*	-
M_m	*Mass fraction of matrix.*	-
V_f	*Volume fraction of fiber.*	-
V_m	*Volume fraction of matrix.*	-

b. Greek Symbols

Symbol	Description	unit
σ_1	Longitudinal stress.	MPa
$(\tau_{12})_{ult}$	In-plane ultimate shear stress	MPa
ϑ_{12}	Poisson's ratio in plane 1-2.	-
τ_{12}	Shear stress in 1-2 plane.	MPa
ε_2^f	Transverse extension of fiber.	-
ε_2^m	Transverse extension of matrix.	-
σ_2	Transverse stress of composite.	MPa
σ_2^f	Transverse stress of fiber.	MPa
σ_2^m	Transverse stress of matrix.	MPa
$(\sigma_m^C)_{ult}$	Ultimate compression of matrix.	MPa
$(\sigma_1^c)_{ult}$	Ultimate longitudinal compressive strength of composite.	MPa
$\left(\varepsilon_{1f}^T\right)_{ult}$	Ultimate longitudinal tension strain of fiber.	-
$\left(\sigma_{1f}^T\right)_{ult}$	Ultimate longitudinal tension stress of fiber.	MPa
$(\sigma_1^T)_{ult}$	Ultimate longitudinal tension strength of composite.	GPa
$(\sigma_2^c)_{ult}$	Ultimate transverse Compressive strength of composite.	MPa
$\left(\sigma_2^T\right)_{ult}$	Ultimate transverse tension strength of composite .	MPa
$(\sigma_m^T)_{ult}$	Ultimate tension stress of matrix.	MPa

Abbreviations

Alphabet Abbreviations

Abbreviations	Meaning
ASTM	American Society for Testing & Materials
C-C	Compression-Compression
CF	Carbon fibers
CFRP	Compositor fiber reinforced polymer
CLT	Classical laminate theory
CM	Composite Materials
CMC	Ceramic Matrix Composite
EP	Epoxy
FEA	Finite element analysis
FRC	Fibers reinforced composite
T-C	Tension-Compression
T-T	Tenssion-Tenssion
WPC	Wood polymer composite

Chapter one
Introduction

Chapter one

Introduction

1.1 General

Composite materials result from combining two or more materials with different physical and chemical properties, and these materials do not lose their properties after combination. Rather, the composite material is enhanced with its properties. The composite material has new properties that are better than if the materials were alone. The choice of components materials depend on the application for which the composite is used. One of these materials is called reinforcement, and it is usually stronger, stiffer, and harder than the second material, which is called the matrix. Composite materials are characterized by low weight, Resistant to environmental conditions, low noise, vibration transmission less than metals, high fatigue strength, low maintenance periods, low thermal expansion, low electrical conductivity, complex parts can be made, low manufacturing cost and high tensile strength may reach four or six times from steel or aluminum based on the type of reinforcement used [1].

The CM nowadays has many applications, and each type of equipment has a special type of composite material. Sports equipment needs lightweight, such as tennis rackets, golf sticks, and other sports equipment, and wind energy needs lightweight turbine blades. Composite materials are also used in aircraft, automobiles, transportation, aerospace equipment, electronic materials, furniture, household goods, medical equipment, military industries, packaging industries, and more [2].

1.2 Classification of composite materials.

Composite materials are often classified based on the matrix or the reinforcing material.

1.2.1 Classification according to the matrix

a. Metal Matrix Composite (MMC)

The MMC is mainly composed of metal or low-density alloys as a matrix such as magnesium, titanium, aluminum, etc., with reinforcement (particles ,fibers, whiskers, etc.) from ceramic or metal materials. The appropriate components are selected according to the required design functions. The MMC is distinguished from other non-reinforced materials by their high stiffness, high specific resistance, good wear resistance, high thermal and electrical conductivity, and reduced linear thermal expansion coefficient, making them .It is involved in many industries, such as the manufacture of parts of military equipment, parts of aircraft engines, gas turbines, and transportation (cars and rail) and other industries [3].

b. Ceramic Matrix Composite (CMC)

Ceramic-composite materials in which the ceramic matrix, such as aluminum oxides, silicon carbides, and silicon nitrates, is reinforced with continuous fibers, particles, or other forms of reinforcement. The CMC has good physical and chemical properties, withstand high temperatures up to 800 degrees, thermal shock resistance, chemical corrosion resistance, and high hardness. However, it is brittle and therefore needs matrix reinforcement to overcome the brittleness, but the crack growth is small compared to materials not reinforced by ceramic matrix. The CMC has many applications, entering aerospace, automotive, aviation, electronic machinery, military equipment, and other applications [4].

c. Polymers Matrix Composite materials (PMC)

The polymer composite material is one of the most widely used composite materials in which the polymer is a matrix because it is cheap and easy to process. It is distinguished from metal and ceramic composites by having low strength, low elastic modulus as in figure 1.1, low shrinkage resistance, can easily penetrate reinforcement and fill voids, and has a suitable chemical resistance. Polymers are divided into thermoset and Thermoplastics polymers.

1. Thermoset polymers, which are materials that cannot be heated above the glass transition temperature because they will char and crack and cannot be recycled again after the form, such as epoxy, polyamide, and others

2. Thermoplastics are moldable and soluble at high temperatures and pressure which can be recycled again after the form, such as polyethylene, polystyrene, and others [5].
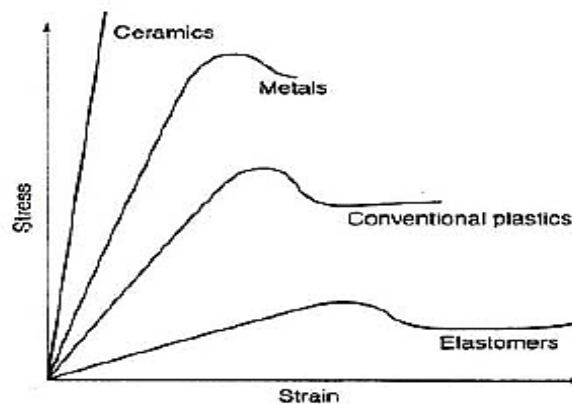
Figure 1.1 Comparison of metal, ceramic, and polymer[5].

1.2.2 Classification according to reinforcement

Composite materials are classified based on the filler into fibers and particles as in Figure 1.2.
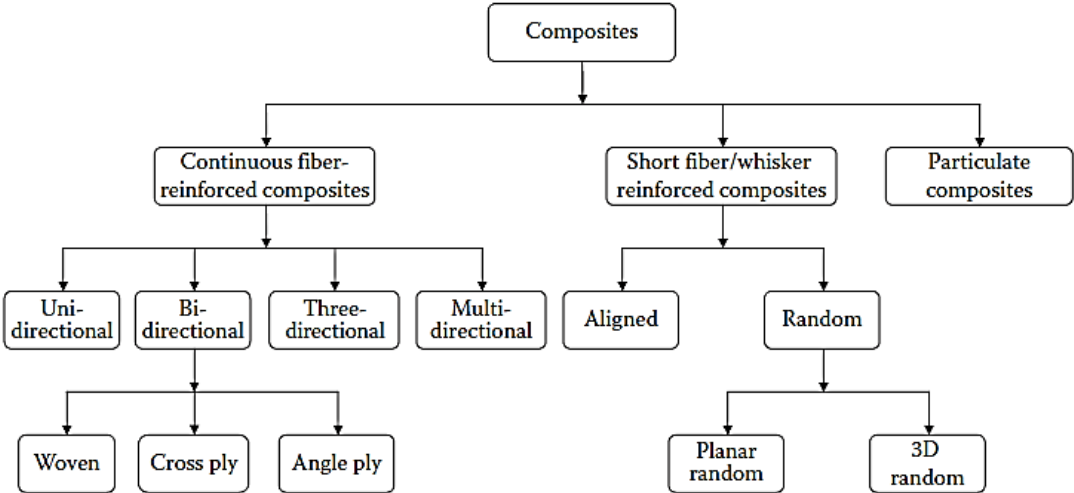
Figure 1.2 classification of CM according to reinforcement[6].

a. Particulate reinforced composites

The reinforcement of this composite is by particles of equal dimensions. These particles give isotropic properties to the composite. The particles may be organic such as rubber powder and cellulose powder, or inorganic particles, such as metal oxides and silica. The Particulate reinforced composites are less effective in strength and fracture resistance than the fibers reinforced composites. It is used in civil engineering applications such as concrete and roads [7].

b. Fibers reinforced composites (FRC)

The fibers are the reinforcing material of the matrix .The fibers can be long and they are called continuous fibers or the fibers are short and they are called dis continuous fibers. The discontinuous fibers must be of sufficient length to allow transfer of the load and avoid the occurrence of cracks that lead to the failure of the composite. The continuous fibers composites are distinguished by their high strength, stiffness, thermal resistance, and abrasion resistance comparison to

discontinuous fibers. The continuous fibers inside the matrix can be unidirectional or bi-unidirectional. The FRC can be manufactured as a single layer or multi-layered of CM .The FRC is called laminate when the layers are made of the same reinforcing fibers in the multilayer composite ,But if two or more types of reinforcing fibers are used, the FRC is called the hybrid composite.

It is easy to control fibers' type, quantity, and direction in these composite. The fibers may be synthetic, such as glass, carbon, basalt, etc., as shown in the figure 1.3. The fatigue strength and shock toughness can be improved by using this type of fiber in the polymer matrix. The fibers may be natural, such as cotton, jute, kenaf,etc. These fibers have recent applications, especially in making environmentally friendly CM [8,9].

Carbon   Basalt   Glass

a: synthetic fibers

Luffa

Banana

Chicken feather

Sisal

Palm

Rice Husk

Cotton

Flax

Jute

Kenaf

Coir

Abaca

b: natural fibers

Figure 1.3 types of fibers [8].

1.3 Motivation behind the present work

The work aims to study the effect of the sequence of layers on the mechanical properties (strength, stiffness, and fatigue) of the unidirectional composite material (carbon/epoxy). The number of layers and the direction of fibers are chosen according to the required mechanical specifications (strength and stiffness) as the failure occurs due to static or cyclic load and may cause the

fibers or the matrix to break and debone them or break the transverse layers. Also, the occurrence of failure in one layer does not mean a complete failure of the composite as the other layers will be able to continue work, unlike the metal materials in which the failure occurs as a crack begins to grow until total failure occurs in a short period. For a unidirectional laminate, the direction of the fibers plays a major role in determining the form and mechanism of failure propagation between the layers. Therefore, it is necessary to study failure theories, choose the appropriate theory, and the effect of layer sequences on mechanical properties.

1.4 Main objectives of the present work

The main objectives of the present work can be summarized as follows:

1. Manufacture a suitable mold with vacuum system to produce a unidirectional laminas (carbon/epoxy) with one layer with different angle fibers i.e. (0º,3º,5º,7º,10º,20º,30º,40º,50º,60º,70º,80º,and 90º).

2. Prepare the above specimens for tensile test according to ASTM3093 standard to find the mechanical properties and compared the results with reference [20].

3. Choose a suitable failure theory for carbon/epoxy lamina after making a comparison between these theories (Maximum stress theory, Maximum strain theory, Tsai-Hill theory, Tsai-Wu theory and Hashin theory) and experimental results for tensile strength of such lamina with different angle
fibers (0 to 90).

4. Study the effect stacking sequence theoretically on the mechanical properties of laminated composite materials with five layers with different angles i.e.(0º,30º,60º,75º,and 90º) using MATLAB program to evaluate the best stacking sequence.

5. Prepare specimens for three stacking sequence to conduct tensile and fatigue tests.

6. Study scanning electron microscope (SEM)analysis of some laminated composite materials to take some information about failure mechanism.

1.5 work limitations

limitations of this work include :

- The mechanical properties of carbon and epoxy

- Using one type of fibers(unidirectional carbon fibers).

- Using one type of polymer matrix materials (epoxy).

- The volume fraction of carbon fiber to epoxy matrix was 30%.

Chapter two

Literature Review

Chapter Two

Literature Review

2.1 General

A lot of researches were presented and many failure theories were developed to evaluate the strength of CM. Some of these researches studied the effect of fiber's orientation within their matrices and mechanical properties. Many of them dealt with static loading while others dealt with dynamic loading and fatigue. On other hand, some researches studied the principles parameters, such as the effect of volume fraction, stress ratio, load frequency ...etc. on the behavior of laminates of CM.

2.2 Effects of laminate's sequence on the mechanical properties under static loading

Many researchers have studied the effect of the stacking sequence of laminate on the mechanical properties of CM. These properties are greatly influenced by the different sequences of layers within a composite material. Finding the appropriate mechanical properties depends on the correct choice of the failure theory for the specific CM. The brief review of some studies that go into this regard are:

Hossain et al. 2012 [10] studied the effect of stacking sequences of jute fiber CM on the tensile properties. They found that the strength differs from laminate to laminate; therefore, they corrected the experimental values by mathematical relationships. Four layers with staking sequences [0/0/0/0], [0/ 45°/-45°/0] and [0/90°/90°/0] were used in their study. Their results showed that in the case of laminates[0/+45°/-45°/0], and [0/0/0/0], the tensile stress parallel to the fibers was higher than the perpendicular tensile stress on the fibers. While no directional difference in tensile strength was observed in the case of using

[0/90°/90°/0]. Their experimental results showed that the jute fibers have tensile properties sensitive to defects, and the tensile strength of CM depends on the tensile strength of the fibers.

Riccio et al. 2014 [11] presented simulations of two different stacking sequences on mechanical behavior under the influence of low-velocity impacts. Highlight on the effect of two different stacking sequences on the mechanical properties due to exposure to low velocity with the use Hashin's criterion to predict damage in numerical simulation by finite element model. In their work, they applied two different levels of absorption energy for a purpose knowing of its effect on stiffness. The sequence $[0/90]_{2S}$ presented less stiffness than the other configuration$[-45/45/90/0]_S$. on the other hand, the sequence of $[0/90]_{2S}$ absorbs higher energy than the previous configuration.

Alves et al. 2016 [12] studied the effect of fibers orientations on the mechanical properties such as modulus of elasticity, density, and tensile strength of a CM reinforced with fibers glass. Orientations used in their study were (0,45,90). They found that density values are inversely proportional with the fiber concentration in the composite where the density in the laminate [0°] was higher than the laminate[45°] and the laminate [90] came last. In addition, maximum tensile load when fibers were oriented by ([0°/0°]) was (287.3 MPa) comparing with that for $\theta = 90°$(110.7 MPa) and with that for $\theta = 45°$(156.3 MPa). The strength increases as the volume fraction of the fibers increases until it reaches 60%. In this case, the matrix cannot wet all the fibers well.

Koc et al. 2016 [13] presented a study on verifying the failure behavior of fiber composite materials under a four-point loading by using the theories (Hoffman, modified quadric surfaces, Tsai-Wu,Hashin, maximum stress, Tsai-Hill, maximum strain, Norris's failure criteria, and quadric surfaces). They designed a four-point bending test so that failure conditions in the intraluminal mode

were more important than delamination failure mode. They performed experiments on $[\theta_{12}]_T$ and $[\theta_3/\theta_3]_S$ layer sequences for fiber angles of 0°, 5°, 15°, 30°, 45°, 60°, 75°, and 90°, used the classical lamination theory (CLT) and the FEM method to simulate the four-point loading to compare the maximum allowable moment resultants from experiments. Their results showed that the quadric surfaces criterion of the configurations better predicts the direction of failure in the plane and out of- the plane load conditions.

Eksi and Genel. 2017 [14] focused on studying the mechanical behavior of epoxy reinforced with different types of fibers (unidirectional carbon fibers, unidirectional glass fibers, carbon woven, glass woven, and aramid woven) under the influence of tensile, compressive and shear loads. They found the tensile strength of unidirectional carbon at an angle of 0 is higher than that of carbon at an angle of 90 by 22.3%, and that the tensile strength of the composite reinforced with unidirectional glass fibers at an angle of 0 is higher than that of with glass fibers at an angle of 90 by 8.3%. The tensile strength of the glass at an angle of 90 was higher than that of the carbon at an angle 90. Also, the tensile strength of the composite reinforced with aramid woven is higher than the tensile strength of the composite reinforced with carbon woven or glass woven. And the composite reinforced with carbon woven gave higher compression and shear strengths than the rest of the composites.

Mohamed et al. 2018 [15] studied the influence of the stacking sequence of laminate CM subjected to multi axial static loading on mechanical properties and damage site. They used three sets of stacking sequence laminates ([45/-45/90/0/90/-45/45],[0/90/45/0/-45/90/0] and [45/-45/0/90/0/90/0])and They used numerical finite element analysis method (FEA)to simulate the composite structure. Based on Hashin's failure criteria, their results showed that the static displacement is decreased as the proportion of layers with a direction of fibers at an angle of 45 is increased. And the best stacking sequence is for

[45/-45/90/0/90/-45/45], when two layers of 45 and -45 oriented plies are at both ends and remaining three layers of 0 and 90 are in between them.

Nagamadhu et al. 2018 [16] studied the effect of stacking sequence, weight fraction, and adhesion between neem wood veneer with epoxy by calculating neem wood polymer composite (WPC) experimentally. They used the hand layup technique method in preparing the samples and treating them by pressure under room temperature and then at high temperature. They carried out many tests to determine the mechanical properties and their results showed improved mechanical properties by increasing the weight fraction of the fiber. The stacking sequence of laminate [0°/0°] shows higher mechanical properties than other sequences (90°/90°, 0°/90°, 45°/90°, 45°/45°).

Zhuang and Wenhong. 2018 [17] studied the failure caused by the spread of damage and the mechanism of spread on the Carbon fiber fabric with epoxy. They used six (0°, 15°, 30°, 45°, 60°, 75°) with eight layers$[0]_8$, $[15]_8$, $[30]_8$, $[45]_8$, $[60]_8$, $[75]_8$ with tensile and a three-point bending tests to determine mechanical properties, Also, to know the behavior of the fracture, they used a scanning electron microscope (SEM) after the three-point bending tests. Their results, through the tensile and bending test, showed that the effect of fiber angle on the mechanical properties of the composite showed similar behavior for both tests, as it showed laminate $[0°]_8$ the best bending and tensile. the failure form was due to the local bulking under bending loading. On the contrary, the laminate $[45°]_8$ were lower mechanical properties for both tests but it had better energy absorption.

Caminero et al. 2019 [18] presented a study on the effect of laminate thickness and the type of lamination technique on the damage, which included three types: unidirectional laminates, Sub laminate angle-ply, and Ply-level angle-ply laminates, all of which are made of carbon and epoxy. They conducted a three-

point flexural test and tensile test on all types. Their results showed a linear behavior of flexural stress for unidirectional samples and that flexural stress and flexural strain decreased and stiffness increased with increasing thickness of the laminates. As for the Sub laminate angle-ply samples, they showed pseudo-ductility due to non-linear behavior and high stress, where the flexural stress increased, and the flexural strain decreased with increasing laminate thickness, whereas the Ply-level angle-ply laminate. It harmed mechanical properties by increasing the thickness of the laminate.

Marzuki et al. 2020 [19] studied the effect fiber's orientation on the flexural properties. They used laminate made of epoxy reinforced with glass fibres, and composed of fibers of different orientation, and composed of fibers of different orientation angles ($\Theta=0°,+45°,-45°,90°$) with six stacking sequences. They take the flexural test according to ASTM D2344, simulate samples using the composite star software program, and note the crack path of each laminate after testing. Their results showed that a stacked sequence of fibers in the ±45 direction shows a transverse and shear crack, which delayed the spread of cracking before it reached a failure state.

Anomani et al. 2020 [20] focused on studying the different failure theories of unidirectional lamina with different angles made of carbon and epoxy. Their results showed that Tsai - Hill theory was the appropriate theory for lamina by comparing experimental and theoretical results where the deviation rate was 17.9%, while Tsai - Wu theory was far from experimental results with a deviation of 60.1%.

Choudhury et al. 2020 [21] presented the effect of angles of fiber orientation of the ply and cross-ply laminated composite beam (graphite /epoxy, glass /epoxy, and their hybrid combinations) under the influence of mechanical and thermal-mechanical load using three boundary conditions (fixed-free, simply

supported, and fixed-fixed). They applied the maximum stress failure criterion, Tsai-WU failure criterion, and Tsai-Hill failure criterion, the foundational failure criterion, to find the strength ratio based on the first ply failure load. The result of their research indicated that the beam consisting of a hybrid compound are economical and lighter than the beam composed of a single type of fiber.

Bate et al. **2020 [22]** studied on the effect of fibers direction on the strength of the unidirectional laminate (carbon/EP)by using a Finite Element Analysis program (FEA) and comparing it is with the experimental results. The angle of the fibers was used 0,45,-45, and 90. The number of laminates of different sequences was obtained up to 1027 of laminates. Their results showed a difference between the theoretical and practical results by more than 20%, and the laminate [0,0,0,0,0] gave The largest loading and bending force in both experimental and experimental results.

2.3 Fatigue behavior of the laminates.

Kadi and Ellyin.1994[23] investigated on the fatigue behavior of a unidirectional composite from glass with epoxy with the stress ratios (0,0.5, -1) and the direction of the different fibers (0°,1 9°, 45°, 71° and 90°) under the influence tension-compression and tension -tension loading. They suggested a strain energy as a criterion for fatigue failure to calculate the effect of the positive and negative stress ratios and orientation fibers angles. The results of their research indicated a breakdown of all the data points obtained from a different set of fiber orientation and stress ratios on a single curve by using the non-dimensional form of this criterion.

Keusch et al. 1998 [24] studied the effect of the interface of differently sized glass fibers on macro mechanical and micromechanical properties and all other parameters being kept constant. They used different sizes of glass fibers. In the first part of their study, tests were calculate the interfacial shear strength and

the interlaminar shear strength to distinguish Fiber/matrix adhesion of unidirectional laminates and the transverse tensile strength. Their research shows that fiber size has a significant effect on the properties. In the second part of their study, the performed test of cross-ply laminates [0/90/90/0] under tension-tension loading with two different sizing's fibers are in the 0° and 90° layers, Where the best fatigue performance was for laminate A (0° and 90° plies with sizing one), followed by C (0° plies with sizing one and 90° plies with sizing four), then B (0° plies with sizing four and 90° plies with sizing one), and finally D (0° and 90° plies with sizing four).

Gamstedt and Talreja .1999 [25] highlighted the fatigue life behavior of two different unidirectional carbon fiber composite, one with epoxy (CF/epoxy), and the other with polyetheretherketone(CF/PEEK) Under the influence of(tensile - tensile) loading, and in the direction of the carbon fiber. They used a quasi-static test for two types to determine mechanical properties and a fatigue test under loading control with a stress ratio of R=0.1 and a frequency of 10 Hz. They discovered in this study, the two composites have the same feature that the damage created from fiber breaks, but there are important differences between them. The composite CF/epoxy has cracks resulting from fiber breakage, and its perpendicular to the direction of the fibers and this is due to the fragility of the composite. The CF/PEEK had a higher resistance to the growth of transverse cracks and damage to the matrix due to shear. Their study suggested choosing Configurations that prevent gradual deboning and breakage of the matrix in the longitudinal direction for better fatigue resistance.

Diao et al. 1999 [26] focused on applying a statistical model to simulate the fatigue behavior of unidirectional lamina subjected to a multi-axial fatigue loading based on the experimental data resulting from the application of uniaxial static load and fatigue load of the unidirectional lamina. They used the statistical model of the off-axis laminates with angles (30,45,and60) to find the

residual strength, fatigue life and static strength. Their results showed good compatibility between the experimental data and applying the statistical model of unidirectional composite lamina under the biaxial fatigue loading to calculate the residual strength and life.

Bezazi et al. 2003[27] presented a study on the mechanical behavior of cross-layers made of epoxy with different fibers as reinforcement (glass fibers, kelvar fibers, and hybrid fibers from glass and kelvar). Where they prepared 9 laminate from (glass/epoxy) with sequences and thickness different by the fiber orientation (0 and 90). They also prepared one laminate of (kelvar/epoxy) with angles (0 and 90), and hybrid laminate from glass and Kevlar fibers. They perform a three point bending test and the fatigue test. Their results showed the effect of the stacking sequences, thickness and orientation of the fibers under static load on the displacement and load values at the rupture of laminate. The hybrid plates showed a non-linear behavior between displacement and load due to Kevlar's fibers. As for the fatigue test, it relied on the R ratio. The laminate whose layers are oriented at an angle of 90 and layers between them are separated by an orientation angle of 0 have better resistance to fatigue.

Kawai. 2004 [28] presented a study on the fatigue behavior of the off-axis laminate of carbon/epoxy and glass/epoxy under the influence of positive mean stresses and constant amplitude loading. He also provided a non-dimensional effective stress that takes into account the stress ratios and the direction of the fibers. He found out "non-dimensional effective stress "as a measure of the strength of brittle materials to describe the nature of fatigue damage, and also by applying the modified non-dimensional effective stress on the Tsai – Hill failure criterion can be obtained theoretical relationship connecting S – N curve for the off-axis fatigue behavior of unidirectional composites. Also, he

found that a general fatigue life equation can be derived by using the fatigue damage mechanic model to create an S-N curve.

Lim et al. 2006 [29] focused on increasing the composite bolted joints' efficiency by using slices with an appropriate stacking sequence. They performed static and fatigue tests on the laminate $[\pm\Theta/0_8]_S$ of bolted joint ($\Theta=$ 45°, 60°, 90°) to determine the mechanical properties, and compared with the properties of the laminate with the stacking sequence of $[0_2/\pm45_3/90_2]_S$ at the same tests, and also used finite element analysis to calculate the stress distributions. Their experimental and analytical results showed that the laminate that has layers stacked in axial direction can be used in bolted join structures under fatigue load at appropriate clamping pressure.

Behrooz et al. 2010[30] studied static behavior and fatigue for (T700-Cycom890 carbon/epoxy) composite laminates ($[0_{10}]$, $[90_{10}]$) and cross-ply ($[0/90]_{4S}$, $[0/90_5/0]$, and$[0/90_4]_S$) for T700/Cycom890 composite laminates with the simulation of the progressive damage model. They did tensile test to determine the static mechanical properties and a fatigue test under tension-tension cyclic loading to determine residual stiffness and strengths. They used the experimental results to find unified fatigue life model, and the constant coefficients of stiffness deterioration, strength deterioration on unidirectional specimens. They conducted experiments on cross-ply specimens under three conditions of different stress and stress ratio(R=0.1). They concluded that the results expected from the model show a good relationship with the experimental.

Shkrieh and Berhooz. 2010 [31] provided a study on fatigue simulation of crossed laminates under (T-T) loading. They developed a progressive damage model by assumptions that on-axis plies are responsible for the laminate's strength reduction and final failure ,while off-axis layers control the stress distribution in the CM. The developed model consists of: stress analysis, failure

17

analysis, gradual stiffness degradation, and strength. It can predict fatigue life for a cross-laminate under different loading conditions. They presented a new unified fatigue life model based on the energy method for unidirectional composite materials under constant amplitude, (T-T), or (C-C) fatigue loadings, and by using the static failure criterion of Sandhu, the proposed model can predict the fatigue life of unidirectional composite materials over the range of positive stress ratios with different fiber orientation angles. Also, the improved model can predict the residual strength and stiffness with limited experimental data and acceptable accuracy.

Katogi et al. 2012 [32] presented a study of a unidirectional composite made of reinforced jute yarns with polylactic acid (PLA) to know its fatigue behavior. They performed the tensile and fatigue tests. They noticed that if the volume fraction increases, the fatigue life increases, and if the number of cycles increased, the strength of fatigue decreased, as the fatigue strength reached 55% of UTS at 10^6 cycles, which is the same percentage for GFRP. The reason is due to the breaking of the jute yarn due to cracks caused by fatigue in the resin PLA.

Brunbauer, and Pinter 2015 [33] presented a study on the combined effect of load type (tension-compression) in quasi-static and the fatigue test (tension-tension and tension-compression) of a unidirectional carbon/epoxy laminate at angles of 0°, 45°, and 90° with different fiber volume content. They noticed that increasing the volume content of the fibers increases the mechanical properties in the T-T fatigue test at all angles. Also, the tensile test of the off-axis samples depends on the volume content of the fibers, and the damage shifts from matrix fracture and debonding between the fibers and the matrix to the pulling of the fibers. As for the increase in the volume content of fibers in the T-C fatigue, the test is useful in improving the fatigue test for angles 45 and 0, while the fatigue strength did not improve for angle 90.

Hosoi et al. 2015 [34] presented a study on the beginning of the transverse crack in cross-ply ($[0/90_4]_S$ and $[0/ 90_6]_S$) by using the fatigue strength properties of unidirectional CFRP in the $[90]_{12}$ direction, where they used the conventional method and proposed(H-K) equation to evaluate the initiation of transverse cracks under fatigue effect in the cross-ply laminate. Their results showed Successful use of the fatigue strength characteristics of the $[90]_{12}$ to predict fatigue life in cross-ply laminates and a good agreement between the analytical and experimental results. Using the equation (H-K), it is preferable to use the analytical method using the equation (H-K)because it predicts conservative fatigue life to transverse crack initiation.

Roundi et.al. 2017 [35] highlight in their study the effect of various stress ratio (R=0.1,R=0.2,R=0.3,R=0.4,R=0.5) and stacking sequence for glass/epoxy composite materials with stacking sequence ($[0_2/90_2]_S$, $[90_2/0_2]_S$, $[0_3/90]_S$, $[90_3/0]_S$) on fatigue behavior. According to Standard ASTM D3039/D3039M, Samples were prepared for static and fatigue tests and finite element analysis to foretell the fatigue behavior. They found that the stacking sequence configuration influences the different static properties such as strain, tensile strength, and Young's modulus, and according to the experimental and numerical data of fatigue where the Most appropriate configuration selection the $[0_3/90]_S$ fiber orientations to achieve the maximum fatigue life. Also, the stress ratio affects fatigue life and stiffness, where fatigue life decreases when the stress ratio is lowered, and stiffness is lower when R=0.1. There is also good agreement between experimental and numerical results.

Nikforooz et al. 2018 [36] provided a study Of the fatigue behavior on glass/polyamide with laminate ($[0]_8$, $[90]_8$, $[0_2/90_2]_S$ and $[0_4/90_4]_S$) and compared it with glass/epoxy from the same formation. They carried out fatigue tests under tension-tension loading. Their results appeared from through the S-N curve that the glass/polyamide laminate $[0]_8$ and the glass/epoxy

laminate $[0]_8$ had been the bilinear trend, and the fatigue resistance of glass/polyamide unidirectional laminate $[0]_8$ is less than the glass/epoxy unidirectional laminate $[0]_8$. The glass/polyamide laminate $[90°]_8$ and glass/epoxy laminate had been a linear trend, and the fatigue resistance of the glass/polyamide laminate $[90°]_8$ less than the glass/epoxy laminate $[90]_8$. In contrast, the cross-layers of glass/polyamide have a fatigue resistance higher than the cross-layers of glass/epoxy. They used an infrared (IR) camera to monitor the temperature rise in the cross-layers of laminates.

Mandegarian et al. 2020[37] focused on creating a model based on the energy failure criterion using in-plane off-axis stress and strain components. This model can predict the fatigue life of carbon/epoxy laminate under different periodic loading conditions (T-T, T-C, and C-C). Their results showed that the model could accurately predict the fatigue life For unidirectional laminates, where the effect of fiber direction and stress ratio was very small; also After entering more test data, the model can be applied to multi-directional laminate, cross-plies, and angle layers, in which the effect of fiber direction and stress ratios diminishes under the three loading conditions. As for composite materials with a complex stacking sequence because many factors affect fatigue life, especially when loading C-C and T-C is dominant.

Bankar et al. 2020 [38] presented a research on the fatigue behavior of a carbon and epoxy composite that has 45 fibers angles by applied constant amplitude (tension-tension), stress ratio (0.1), and frequency 5Hz. They applied the non-destructive test to estimate fatigue life and used the curve structure technique to develop an experimental fatigue life model. Their results showed that the non-destructive test, the model testing, and reducing the natural frequency could reduce the total stiffness.

Padmaraj et al. 2020[39] presented a study on the fatigue behavior of glass/epoxy laminate with stacking sequence $[0/90/+45/-45]_S$ under the influence of constant (tension-tension) load, stress ratio 0.1, and frequency 3Hz. They conducted a scanning electron microscope test on the fracture region to see the shape of the damage. Their results showed the growth of the damage due to the deterioration of the stiffness in the initial fatigue. With the loading of the material, the stiffness is decreased until it reaches a constant deterioration that leads to the failure of the material. Also, the images showed the cracking of the fibers.

2.4 Concluding Remarks

By reviewing the above literature, we conclude the following:

No.	Materials used	Parameters studied
[10]	Epoxy reinforced by jute fiber composite materials	The effect of sequence stacking on mechanical properties and SEM
[12]	Epoxy reinforced by glass fiber composite materials	The mechanical properties such as modulus of elasticity, density, and tensile
[14]	Unidirectional and Woven Carbon, Glass and Aramid Fiber Reinforced Epoxy Composites	Mechanical behavior of laminate under tensile, compressive and shear loads
[16]	The neem wood veneer with epoxy	The effect of sequence stacking and weight fraction on mechanical properties
[17]	The woven carbon fiber/epoxy laminates	The failure caused by the spread of damage and the mechanism
[18]	Three types of laminate (carbon/epoxy): unidirectional laminates, Sub laminate angle-ply, and Ply-level angle-ply	The effect of laminate thickness and the type of lamination technique on the damage

[21]	Graphite /epoxy, glass /epoxy, and their hybrid combinations	The effect of angles of fiber orientation of the ply and cross-ply laminated composite beam
[22]	The unidirectional laminate (carbon/EP)	The effect of fibers orientation and sequence on mechanical properties
[23]	Unidirectional composite from glass with epoxy	The effect stress ratios (0,0.5, -1) and fibers orientation (0°,1 9°, 45°, 71° and 90°) on fatigue behavior
[25]	The two different unidirectional carbon fiber composite, one with epoxy (CF/epoxy), and the other withpolyetheretherketone(CF/PEEK)	The effect of type composite on fatigue life
[30]	T700/Cycom890 carbon/epoxy) composite laminates	The effect of stacking sequence on fatigue behavior
[33]	Unidirectional carbon/epoxy laminate	Effect of load type (tension-compression) and volume fibers on the fatigue test
[36]	The glass/epoxy composite materials	The effect of stacking sequence and stress ratio on fatigue behavior
[37]	The glass/polyamide laminate and glass/epoxy laminate	The effect of type of laminate and the type of sequence on fatigue

The present study is differ from the published work by study the mechanical properties of unidirectional carbon fiber reinforced with epoxy resin with one layer for different angles (0°,3°,5°,7°,10°,20°,30°,40°,50°,60°,70°,80°,and 90°) with volume fraction 30% and compare the results with five failure theories to choose a suitable theory for a lamina, then studying the effect of stacking

sequence of five layers with different fibers orientation i.e. .(0º,30º,60º,75º,and 90º) on mechanical properties to choose the best stacking sequence of fibers.

Fatigue and tensile tests will be conducted After choosing three stacking sequences of laminates with different theoretical tensile strength, one of them represents a low, medium and high tensile value, finally scanning electron microscope analysis was performed to show some information about CM failure.

Chapter Three
Theoretical Analysis

Chapter three

Theoretical analysis

3.1 introduction

The main driver behind the advancement of composite materials was the increasing need for materials with higher mechanical properties and lowered specific weight. One of the essential advantages of laminated materials is their ability to direct the sheets appropriately or choose the appropriate stacking sequence configurations to obtain the required mechanical properties. Fiber-reinforced polymer matrix CM has received widespread attention due to its applications in automobiles, aero planes, marine and civil structures.

Stiffness and (strength /weight ratio) are most of the required properties. The stiffness of the composite is required not to be very high in specific applications such as shock absorbers and springs. Design and analysis of any laminated CM require a good knowledge of the mechanical properties of the lamina. If the lamina is unidirectional, the fiber's orientation will highly affect the overall mechanical properties. Elastic coefficients of either fibers and matrix, the coefficients of moisture expansion, and the proper selection of the failure theory will be significant in determining the mechanical properties of the CM.

3.2 Materials
3.2.1. Matrix Materials

The matrix material is usually homogeneous, isotropic, and continuous. It may be ceramic, polymer, or metal. It performs many functions [40].

- It directs the fibers in the correct direction and maintains their spacing.
- The matrix protects the fibers from corrosion and environmental conditions

- The matrix transfers the load from the matrix to the fibers during the shear loading at the interface.

- Increase the toughness of the composite as a ceramic matrix.

Epoxy matrix, which is used in this work, is one of the widely used types of polymers because it has many advantages [41]:

- High strength and corrosion resistance

- Good resistance to fatigue and creep

- Low shrinkage during hardening

- Good adhesion with many fibers

- Good electrical properties

- Environmentally friendly

- Easy processing

3.2.2 Fibers Materials

Fibers are either continuous or discontinuous, and this depends on the length of the fibers concerning their diameter. If the fibers are long, it has a high aspect ratio(l/d); on the contrary, the fibers will be discontinuous. The continuous fibers can be in different directions like unidirectional fibers , helical windy, and woven fibers. As the figure 3.1[42].
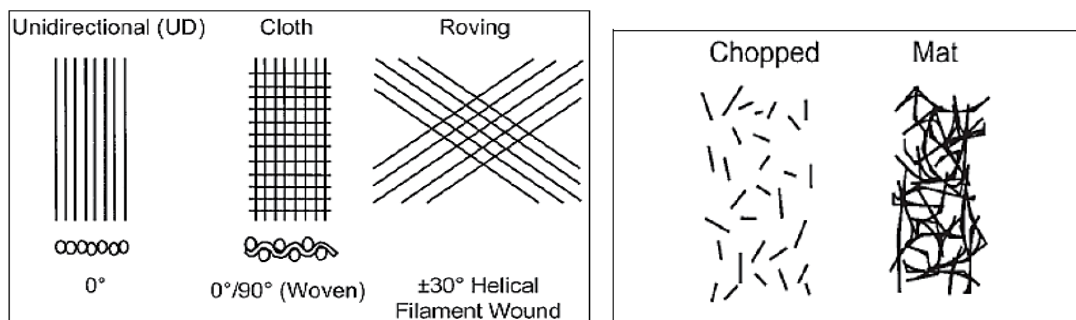
a) continuous fiber   b) Discontinuous fiber

Figure 3.1type of fiber [42]

In this work, unidirectional carbon fiber will reinforce the epoxy. Carbon fibers have good properties such as high strength, stiffness, lightweight. They are used in applications requiring high temperature, chemical inertness, and good electricity and thermal conductivity [43].

3.3 Micromechanics of lamina

The lamina consists of parallel fibers by equal distances between them and immersed in the matrix material, and these materials are mostly homogeneous. The lamina is quasi-homogeneous and anisotropic. Figure 3.2 shows the coordinates of the lamina, where the coordinates x, y, and z are called lamina coordinate or global coordinates, and the coordinates 1, 2, and 3 are called the local coordinates or principal coordinate.

The fibers' inclination angle (θ) from the x-axis is called fibers orientation, which is positive if measured counterclockwise, and θ is negative if measured clockwise. The z and 3 axes are positive at the top of the lamina and negative at the bottom.

Axis-1 runs parallel to the direction of fibers, and it is called longitudinal direction.

Axis-2 is perpendicular to axis-1and is called transverse direction

Axis-3 is perpendicular to axis-1 and axis-2 and is called transverse direction.

The laminate consists of several layers (lamina), which have different fiber orientations that give its good mechanical properties for laminate [44].
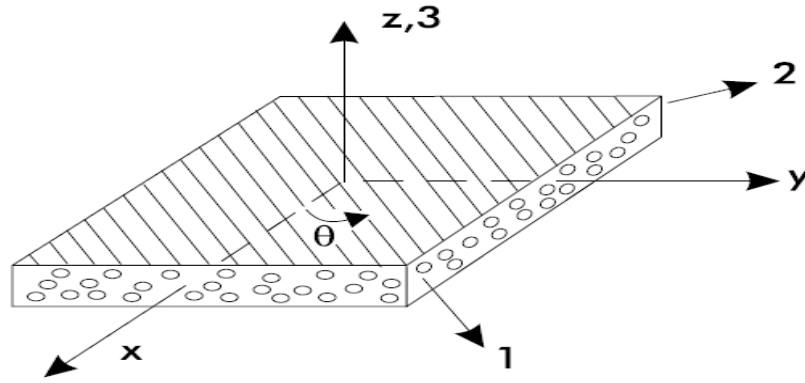
Figure 3.2 global and local axes of laminate[44].

3.3.1 The rule of mixture

The properties of the composite are determined by knowing the individual properties of its constitutes, such as volume fractions, mass fractions, and densities. The rule of the mixture is one of the approximate and straightforward methods used to find the mechanical properties of the lamina, which can be applied to the micro-mechanics of composites. It is based on several assumptions: The constitutes of the lamina (matrix and fibers) are homogeneous, isotropic, linearly elastic, the fibers are evenly distributed, and the bond between the matrix and the fibers is perfect [45].

3.3.2 Volume Fractions of the lamina

As for the uniform distribution of the fibers, it is possible to directly calculate the volume fraction of the fibers according to the shape [46].

$$v_f + v_m = v_c \tag{3.1}$$

Where $v_{f,m,c}$ The volume and the subscribe f, m, and c correspond to fibers, matrix, and composite materials.

$$V_f = \frac{v_f}{v_c} \quad , \quad V_m = \frac{v_m}{v_c} \tag{3.2}$$

From Equation (3.1)

$$V_f + V_m = 1 \tag{3.3}$$

3.3.3 Mass fraction of lamina

Mass fraction of matrix is the ratio of the mass matrix to the mass of CM, and the mass fraction of fibers is the ratio of the mass fibers to the mass of CM [46].

$$w_f + w_m = w_c \tag{3.4}$$

$$W_f = \frac{w_f}{w_c} \ , \ W_m = \frac{w_m}{w_c} \tag{3.5}$$

Where $w_{f,m,c}$ is the mass of the fibers, matrix, and composite materials, respectively

$$W_f + W_m = 1 \tag{3.6}$$

3.3.4 Density

Derivation of density analytically. The mass of composite w_c equal the sum mass of fibers w_f and mass of matrix w_m [46].

$$w_f = \rho_f v_f \ , w_m = \rho_m v_m \ , \ w_c = \rho_c v_c \tag{3.7}$$

By substituting equation (3.7) into equation (3.4) to obtain this equation.

$$\rho_c v_c = \rho_f v_f + \rho_m v_m \tag{3.8}$$

$$\rho_c = \rho_f V_f + \rho_m V_m \tag{3.9}$$

3.3.5 Longitudinal modulus of CM

The material strength approach is used to calculate the stiffness parameters. The model in figure 3.3 assumes the fibers are in the lower part of the model, and the matrix is in the upper part. The model is subjected to a uniaxial load (F). that the longitudinal extensions in the fiber, matrix and composite are equal (iso-strain) [47].
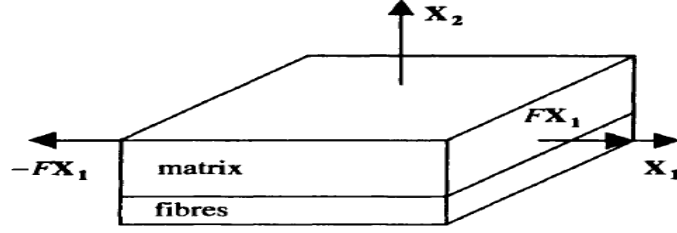
Figure 3.3 the geometry shape of the volume element under effect load in x1 direction[47].

$(\varepsilon_c = \varepsilon_f = \varepsilon_m)$

$$\varepsilon_c = \frac{\sigma_c}{E_C}, \varepsilon_f = \frac{\sigma_f}{E_f}, \varepsilon_m = \frac{\sigma_m}{E_m} \tag{3.10}$$

In iso-strain case, The load applied to the composite (F_C) is approximately equal to the sum of the fibers load (F_f) and matrix load (F_m)

$$F_C = F_f + F_m \tag{3.11}$$

$$\sigma_c A_c = \sigma_f A_f + \sigma_m A_m \tag{3.12}$$

$$V_f = \frac{A_f l}{A_c l}, \quad V_m = \frac{A_m}{A_c} \tag{3.13}$$

Where l is the length geometric of the model element.

by Substitute, the equations (3.10) and (3.13) into Equation (3.12)

$$E_c = E_1 = E_f V_f + E_m V_m \tag{3.14}$$

3.3.6 Major Poisson's Ratio

The primary Poisson's ratio is defined as the negative transverse strain to the longitudinal strain under uniaxial loading in the fiber direction[47].

As the figure (3.3)

$$\varepsilon_2^f = -\vartheta_f \varepsilon_1 \quad , \quad \varepsilon_2^m = -\vartheta_m \varepsilon_1 \tag{3.15}$$

Where ϑ_f and ϑ_m represent Poisson's ratio of fibers and matrix, respectively.

$$\Delta_c = \Delta_f + \Delta_m \tag{3.16}$$

Where $\Delta_c, \Delta_f, \Delta_m$ are the change of thickness in composite, fibers, and matrix, respectively.

$$\Delta_c = t_f \varepsilon_2^f + t_m \varepsilon_2^m \tag{3.17}$$

Where t_f and t_m Are the thickness of the fibers and matrix, respectively.

$$V_f = \frac{t_f bl}{t_{cbl}} \quad \text{and} \quad V_m = \frac{t_m bl}{t_c bl} \tag{3.18}$$

Where b is the width of the model element.

Substitute equations (3.15) and (3.18) in Equation (3.17).

$$\varepsilon_2 = \frac{\Delta_c}{t_c} = -(V_f \vartheta_f + V_m \vartheta_m)\varepsilon_1 \tag{3.19}$$

$$\vartheta_{12} = (V_f \vartheta_f + V_m \vartheta_m) \tag{3.20}$$

3.3.7 Transverse modulus of CM

The model in figure 3.4, When a composite material is loaded in the transverse direction of the fiber, the stresses in the fiber, matrix, and composite are equal (iso-stress) [47].
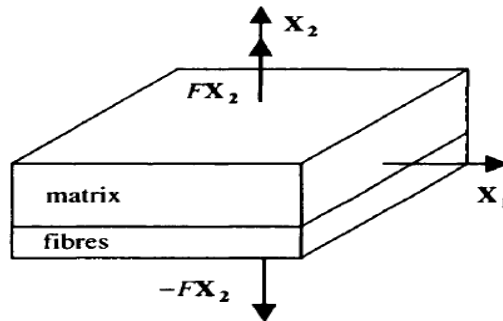
Figure 3.4 the geometry shape of the volume element under effect load in x2 direction[47].

$$\sigma_c = \sigma_2^f = \sigma_2^m \tag{3.21}$$

The composite elongation (Δ_c) is equal to the sum elongation of fibers (Δ_f) and elongation of matrix (Δ_m)

$$\Delta_c = \Delta_f + \Delta_m \tag{3.22}$$

$$\Delta_c = t_f \varepsilon_2^f + t_m \varepsilon_2^m \tag{3.23}$$

$$\varepsilon_2 = \frac{\Delta_c}{t_c} = -(V_f \varepsilon_2^f + V_m \varepsilon_2^m) \tag{3.24}$$

$$\frac{\sigma_c}{E_2} = V_f \frac{\sigma_2^f}{E_f} + \frac{\sigma_2^m}{E_m} V_m \tag{3.25}$$

$$\frac{1}{E_2} = \frac{V_f}{E_f} + \frac{V_m}{E_m} \tag{3.26}$$

3.3.8 In-Plane Shear Modulus

The model is subject to shear stress (τ_{12}) as shown in figure 3.5. It is assumed that the fibers, the matrix, and composite shear stresses are equal [47].
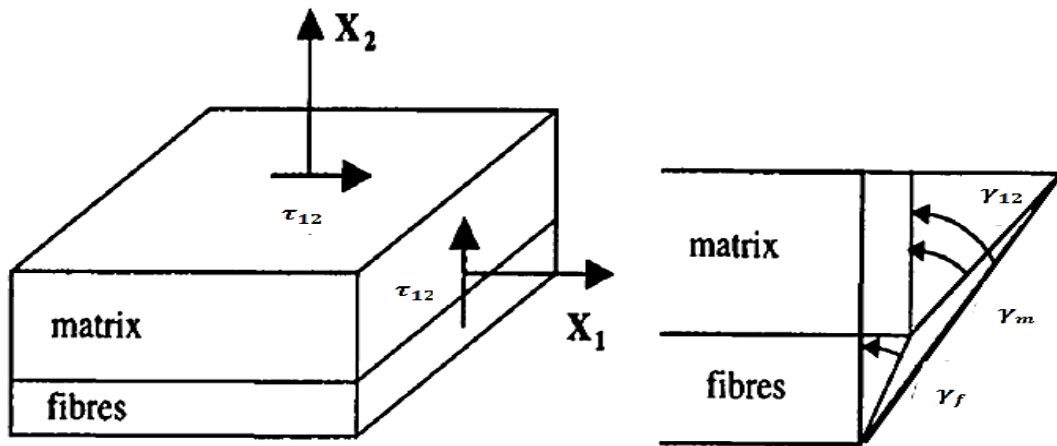
Figure 3.5 the geometry shape of the volume element under effect shear load in (x1,x2) plane [47].

$$\tau_{12} = \tau_f = \tau_m$$

$$\gamma_f = \frac{\tau_f}{G_f} \quad , \quad \gamma_m = \frac{\tau_m}{G_m} \tag{3.27}$$

Where γ_f , γ_m are represent the shear strain of fibers and matrix

$$\delta_c = \delta_f + \delta_m \tag{3.28}$$

$$\delta_f = t_f \gamma_f, \quad \delta_m = t_m \gamma_m \tag{3.29}$$

$$\gamma_c t_c = t_f \gamma_f + t_m \gamma_m \tag{3.30}$$

$$\frac{1}{G_{12}} = \frac{V_f}{G_f} + \frac{V_m}{G_m} \tag{3.31}$$

3.3.9 Ultimate longitudinal tensile strength

The qualities of its components (fibers and matrix), as well as the bonding between them, determine the unidirectional Lamina's failure. Fiber fracture, fiber tugging, matrix cracking, and de-bonding between the fibers and the matrix are potential unidirectional lamina failures when subjected to a longitudinal tensile load.

To calculate the strength of the lamina, it is assumed that the fibers and the matrix are homogeneous, isotropic, and linearly elastic.

There are two possibilities for the maximum strain fiber and the maximum strain matrix[48].

Case 1 :$\varepsilon_f < \varepsilon_m$ as shown in figure 3.6.

$$\sigma_{1\,\text{ult}}^{\text{T}} = \left(\sigma_{1f}^{\text{T}}\right)_{\text{ult}} V_f + \left(\varepsilon_{1f}^{\text{T}}\right)_{\text{ult}} E_m (1 - V_f) \tag{3.32}$$
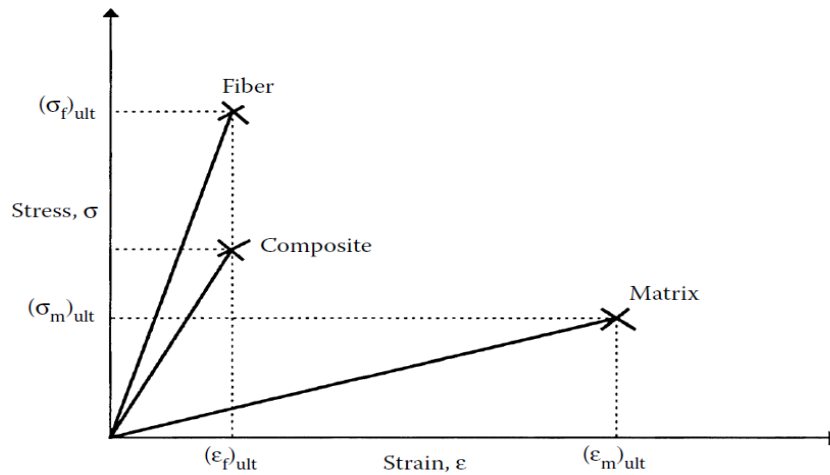
Figure 3.6 the stress-strain diagram of the fiber, the matrix, and the
unidirectional lamina consisting of them[48].

- **Case 2: $\varepsilon_f > \varepsilon_m$**

$$(\sigma_1^T)_{ult} = (\varepsilon_m^T)_{ult} E_{1f} V_f + (\sigma_m^T)_{ult}(1 - V_f) \qquad (3.33)$$

3.3.10 Ultimate longitudinal compressive strength

The strength of unidirectional lamina under longitudinal compression differs
from under longitudinal tension, becoming more complex. Therefore the
typical Failure is created as in figure 3.7 [48].
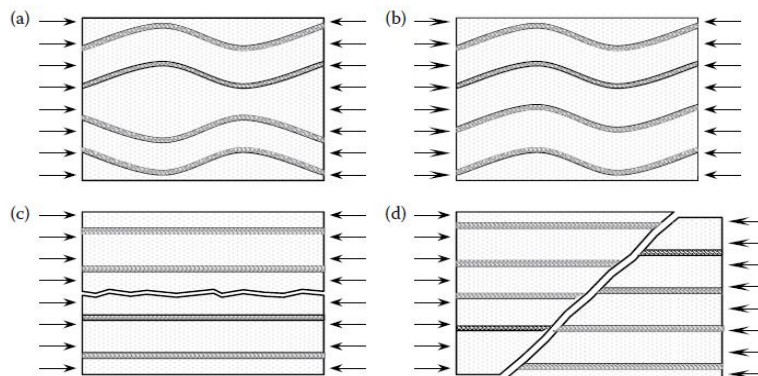
Figure 3.7 failure modes of lamina under longitudinal compression[48].

a. Micro-buckling of fibers and extension in matrix

$$(\sigma_1^C)_{\text{ult}} \approx 2V_f \sqrt{\frac{V_f E_{1f} E_m}{3(1-V_f)}} \tag{3.34}$$

b. Micro-buckling of fibers or the shear mode to which the matrix is sheared.

$$(\sigma_1^C)_{\text{ult}} \approx \frac{G_m}{1-V_f} \tag{3.35}$$

c. Fracture of matrix or fiber–matrix bond due to tensile strains in the matrix

$$\varepsilon_2^T = v_{12}\varepsilon_1^C = \frac{v_{12}(\sigma_1^C)_{ult}}{E_1} \tag{3.36}$$

d. Shear failure in CM

$$(\sigma_1^C)_{\text{ult}} = 2(\tau_f)_{ult}[V_f + \frac{E_m}{E_{1f}}(1-V_f)] \tag{3.37}$$

The designer must choose the lowest ultimate stress values for
the composite to be in a safe condition.

3.3.11 In-plane ultimate shear strength

The procedure of finding shear modulus is applied to calculate the ultimate
shear strength [48].

The shear stress in fibers and matrix are equal

$$\gamma_m G_m = \gamma_f G_f \tag{3.38}$$

by substituting the Equation (3.38) in Equation (3.30) to obtain.

$$(\gamma_{12})_{\text{ult}} = [1 + \left(\frac{G_m}{G_f} - 1\right)V_f](\gamma_m)_{\text{ult}} \tag{3.39}$$

$$(\tau_{12})_{\text{ult}} = G_{12}(\gamma_{12})_{\text{ult}} \tag{3.40}$$

3.3.12 Ultimate transverse Tensile Strength

The tensile strength of the unidirectional lamina is given[54].

$$(\sigma_2^T)_{ult} = E_2(\varepsilon_2^T)_{\text{ult}} \tag{3.41}$$

Can be used the empirical relationship

$$(\varepsilon_2^T)_{ult} = (\varepsilon_m^T)_{ult}(1 - V_f^{\frac{1}{3}}) \tag{3.42}$$

3.3.13 Ultimate transverse Compressive strength

Failure can occur due to failure of the interface between the matrix and fiber, failure of matrix shear or matrix compression, and failure modes may occur together as in the equation (3.44) for the transverse tensile strength [48].

$$(\sigma_2^c)_{ult} = E_2(\varepsilon_2^c)_{ult} \tag{3.43}$$

$$(\sigma_2^c)_{ult} = E_2[1 + \left(\frac{E_m}{E_f} - 1\right)V_f](\varepsilon_m^c)_{ult} \tag{3.44}$$

If the cross-section of the fibers is circular and the distribution is in the form of a square array, the following equation can be used.

$$\left(\sigma_2^C\right)_{ult} = (\sigma_m^C)_{ult}\left[1 - 2\sqrt{\frac{v_f}{\pi}}\right] \tag{3.45}$$

3.4 Macro mechanics of lamina

The state of stress in anisotropic materials can be shown by taking a small element in the form of a cube that has equal and parallel sides, as in figure 3.8, where the stresses (σ_{ij}) (i,j=1,2,6) are nine. Similarly, the state of strain can be represented by nine components. The components of the strain (ε_{ij}) are related to stress by Hooke's law [49].

$$
\begin{bmatrix} \sigma_{11} \\ \sigma_{22} \\ \sigma_{33} \\ \sigma_{23} \\ \sigma_{31} \\ \sigma_{12} \\ \sigma_{32} \\ \sigma_{13} \\ \sigma_{21} \end{bmatrix} =
$$

$$
\begin{bmatrix}
C_{1111} & C_{1122} & C_{1133} & C_{1123} & C_{1131} & C_{1112} & C_{1132} & C_{1113} & C_{1121} \\
C_{2211} & C_{2222} & C_{2233} & C_{2223} & C_{2231} & C_{2212} & C_{2232} & C_{2213} & C_{2221} \\
C_{3311} & C_{3322} & C_{3333} & C_{3323} & C_{3331} & C_{3312} & C_{3332} & C_{3313} & C_{3321} \\
C_{2311} & C_{2322} & C_{2333} & C_{2323} & C_{2331} & C_{2312} & C_{2332} & C_{2313} & C_{2321} \\
C_{3111} & C_{3122} & C_{3133} & C_{3123} & C_{3131} & C_{3112} & C_{3132} & C_{3113} & C_{3121} \\
C_{1211} & C_{1222} & C_{1233} & C_{1223} & C_{1231} & C_{1212} & C_{1232} & C_{1213} & C_{1221} \\
C_{3211} & C_{3222} & C_{3233} & C_{3223} & C_{3231} & C_{3212} & C_{3232} & C_{3213} & C_{3221} \\
C_{1311} & C_{3122} & C_{3133} & C_{3123} & C_{1331} & C_{1312} & C_{1332} & C_{1313} & C_{1321} \\
C_{2111} & C_{2122} & C_{2133} & C_{2123} & C_{2131} & C_{2131} & C_{2132} & C_{2113} & C_{2121}
\end{bmatrix}
\begin{bmatrix} \varepsilon_{11} \\ \varepsilon_{22} \\ \varepsilon_{33} \\ \varepsilon_{23} \\ \varepsilon_{31} \\ \varepsilon_{12} \\ \varepsilon_{32} \\ \varepsilon_{13} \\ \varepsilon_{21} \end{bmatrix} .(3.46)
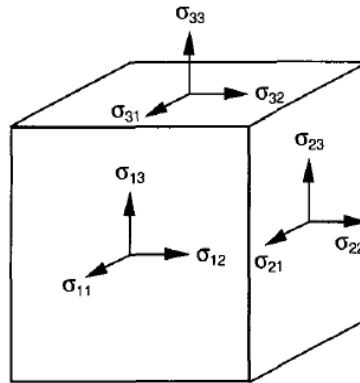$$

Figure 3.8 state of stress at small cube element[49].

An anisotropic material has eighty-one elasticity constants, reduced to thirty-six due to the symmetry between the stresses and strain tensors.

$$\begin{bmatrix} \sigma_1 \\ \sigma_2 \\ \sigma_3 \\ \tau_{12} \\ \tau_{23} \\ \tau_{13} \end{bmatrix} = \begin{bmatrix} C_{11} & C_{12} & C_{13} & C_{14} & C_{15} & C_{16} \\ C_{21} & C_{22} & C_{23} & C_{24} & C_{25} & C_{26} \\ C_{31} & C_{32} & C_{33} & C_{34} & C_{35} & C_{36} \\ C_{41} & C_{42} & C_{43} & C_{44} & C_{45} & C_{46} \\ C_{51} & C_{52} & C_{53} & C_{54} & C_{55} & C_{56} \\ C_{61} & C_{61} & C_{63} & C_{64} & C_{65} & C_{66} \end{bmatrix} \begin{bmatrix} \varepsilon_1 \\ \varepsilon_2 \\ \varepsilon_3 \\ \gamma_{12} \\ \gamma_{23} \\ \gamma_{13} \end{bmatrix} \qquad (3.47)$$

Due to the effect of an external force on the body. Work is produced translated into recoverable strain energy[49].

The strain energy per unit volume $= W = \frac{1}{2} \sum_{1}^{6} \sigma_i \varepsilon_i$ $\qquad (3.48)$

Substitute for Hooke's law

$$w = \frac{1}{2} \sum_{i=1}^{6} \sum_{j=1}^{6} C_{ij} \varepsilon_i \varepsilon_j \qquad (3.49)$$

by differentiating

$$\sigma_i = \frac{\partial w}{\partial \varepsilon_i} = C_{ij} \varepsilon_j \qquad (3.50)$$

by Making a differential again

$$C_{ij} = \frac{\partial^2 w}{\partial \varepsilon_i \partial \varepsilon_j} \qquad (3.51)$$

In the same way, by reversing the differential order. The result is obtained.

$$C_{ji} = \frac{\partial^2 w}{\partial \varepsilon_j \partial \varepsilon_i} \qquad (3.52)$$

This leads to

$$C_{ij} = C_{ji} \qquad (3.53)$$

This means that the stiffness matrix is symmetric. Therefore, the number of independent constants for the anisotropic material becomes 21.

3.4.1 The relation between stress-strain for the unidirectional lamina

In most applications of CM, the laminates are thin and loaded in the plane, so the unidirectional lamina can be considered under the condition of the plane stress so that all the stresses out-of-plane are equal to zero [49].

Thus, The equation (3.47) is represented by the following.

$$\begin{bmatrix} \sigma_1 \\ \sigma_2 \\ 0 \\ 0 \\ 0 \\ \tau_{12} \end{bmatrix} = \begin{bmatrix} C_{11} & C_{12} & C_{13} & 0 & 0 & 0 \\ C_{12} & C_{22} & C_{23} & 0 & 0 & 0 \\ C_{13} & C_{23} & C_{33} & 0 & 0 & 0 \\ 0 & 0 & 0 & C_{44} & 0 & 0 \\ 0 & 0 & 0 & 0 & C_{55} & 0 \\ 0 & 0 & 0 & 0 & 0 & C_{66} \end{bmatrix} \begin{bmatrix} \varepsilon_1 \\ \varepsilon_2 \\ \varepsilon_3 \\ 0 \\ 0 \\ \gamma_{12} \end{bmatrix} \tag{3.54}$$

$$\left. \begin{aligned} \sigma_1 &= C_{11}\varepsilon_1 + C_{12}\varepsilon_2 + C_{13}\varepsilon_3 \\ \sigma_2 &= C_{12}\varepsilon_1 + C_{22}\varepsilon_2 + C_{23}\varepsilon_3 \\ 0 &= C_{13}\varepsilon_1 + C_{23}\varepsilon_2 + C_{33}\varepsilon_3 \\ \gamma_{13} &= \gamma_{23} = 0 \\ \tau_{12} &= C_{66}\gamma_{12} \end{aligned} \right\} \tag{3.55}$$

by simplifying the Equations.

$$\left. \begin{aligned} \sigma_1 &= \left(C_{11} - \frac{C_{13}C_{13}}{C_{33}} \right)\varepsilon_1 + \left(C_{12} - \frac{C_{13}C_{23}}{C_{33}} \right)\varepsilon_2 \\ \sigma_1 &= Q_{11}\varepsilon_1 + Q_{12}\varepsilon_2 \\ \sigma_2 &= \left(C_{12} - \frac{C_{13}C_{23}}{C_{33}} \right)\varepsilon_1 + \left(C_{22} - \frac{C_{23}C_{23}}{C_{33}} \right)\varepsilon_2 \\ \sigma_2 &= Q_{12}\varepsilon_1 + Q_{22}\varepsilon_2 \end{aligned} \right\} \tag{3.56}$$

$$\tau_{12} = C_{66}\gamma_{13} = Q_{66}\gamma_{12}$$

$$\begin{bmatrix} \sigma_1 \\ \sigma_2 \\ \tau_{12} \end{bmatrix} = \begin{bmatrix} Q_{11} & Q_{12} & 0 \\ Q_{12} & Q_{22} & 0 \\ 0 & 0 & Q_{66} \end{bmatrix} \begin{bmatrix} \varepsilon_1 \\ \varepsilon_2 \\ \gamma_{12} \end{bmatrix} \tag{3.57}$$

$$Q_{11} = \frac{E_1}{1 - \nu_{21}\nu_{12}}, \quad Q_{12} = \frac{\nu_{12}E_2}{1 - \nu_{21}\nu_{12}}, \quad Q_{22} = \frac{E_2}{1 - \nu_{21}\nu_{12}}, \quad Q_{66} = G_{12} \tag{3.58}$$

Where $[Q_{ij}]$ is stiffness matrix.

3.4.2 Transformation of stress and strain (two-dimensional)

As in figure 3.1, the loading axes (x, y) do not coincide with the unidirectional lamina's principal axes (1,2). These axes are related to the transformation relationship[49].

The global and local stress from the following relationship.

$$\begin{bmatrix} \sigma_1 \\ \sigma_2 \\ \tau_{12} \end{bmatrix} = [T] \begin{bmatrix} \sigma_x \\ \sigma_y \\ \tau_{xy} \end{bmatrix} \tag{3.59}$$

Also, the global and local strain from the following relationship.

$$\begin{bmatrix} \varepsilon_x \\ \varepsilon_y \\ \gamma_{xy/2} \end{bmatrix} = [T] \begin{bmatrix} \varepsilon_1 \\ \varepsilon_2 \\ \gamma_{12/2} \end{bmatrix} \tag{3.60}$$

Where $[T]$ is called the transformation matrix[50].

$$[T] = \begin{bmatrix} m^2 & n^2 & 2nm \\ n^2 & m^2 & -2nm \\ -nm & nm & m^2 - n^2 \end{bmatrix} \tag{3.61}$$

Where ,n=sinθ , m=cosθ

by substituting the equation (3.59) and (3.60) in equation (3.57).

The following equation is obtained :

$$\begin{bmatrix} \sigma_x \\ \sigma_y \\ \tau_{xy} \end{bmatrix} = \begin{bmatrix} \bar{Q}_{11} & \bar{Q}_{12} & \bar{Q}_{16} \\ \bar{Q}_{12} & \bar{Q}_{22} & \bar{Q}_{26} \\ \bar{Q}_{16} & \bar{Q}_{16} & \bar{Q}_{66} \end{bmatrix} \begin{bmatrix} \varepsilon_x \\ \varepsilon_y \\ Y_{xy} \end{bmatrix} \tag{3.62}$$

Where $[\bar{Q}ij]$ is the elements of the transformed reduced stiffness matrix.

$$\bar{Q}_{11} = Q_{11}\, m^4 + Q_{22}\, n^4 + 2\,(Q_{12} + 2Q_{66})\, m^2\, n^2 ,$$

$$\bar{Q}_{12} = (Q_{11} + Q_{22} - 4\, Q_{66})\, n^2\, m^2 + Q_{12}\, (m^4 + n^4) ,$$

$$\bar{Q}_{22} = Q_{11}\, n^4 + Q_{22}\, m^4 + 2\,(Q_{12} + 2Q_{66})\, n^2\, m^2 , \tag{3.63}$$

$$\bar{Q}_{16} = (Q_{11} - Q_{12} - 2\, Q_{66})\, mn^3 - (Q_{22} - Q_{12} - 2\, Q_{66})\, m^3\, n ,$$

$$\bar{Q}_{26} = (Q_{11} - Q_{12} - 2\, Q_{66})\, m\, n^3 - (Q_{22} - Q_{12} - 2\, Q_{66})\, n^3\, m ,$$

$$\bar{Q}_{66} = (Q_{11} + Q_{22} - 2\, Q_{12} - 2Q_{66})\, n^2\, m^2 + Q_{66}\, (n^4 + m^4)$$

3.4.3 The strength of off-axis lamina

The strengths for off-axis lamina axes can be converted to the stresses on the principle axes as the following equations[49].
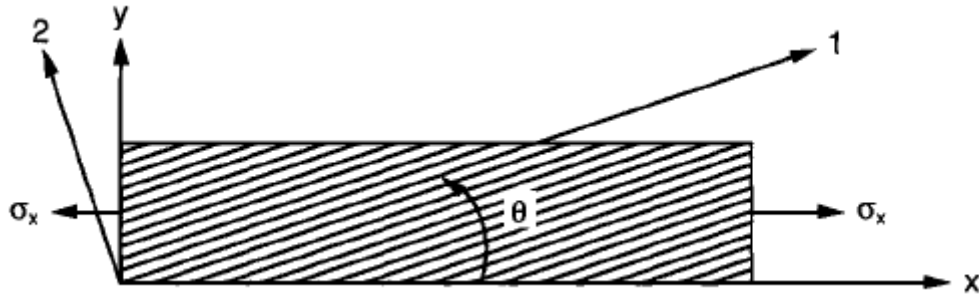
Figure 3.9 loading the lamina in the x-direction

$$\sigma_1 = \sigma_x cos^2\theta$$
$$\sigma_2 = \sigma_x sin^2\theta$$
$$\tau_{12} = -\sigma_x cos\,\theta sin\,\theta$$

(3.64)

Strength ratio=$\dfrac{\text{Maximum load applied}}{\text{applied load}} = \dfrac{\text{ultimate strength}}{\text{applied stress}}$

If SR=1 means the failure load or SR>1, the lamina is safe can be increased the applied load or SR<1, which means the lamina is unsafe. Therefore the applied stress must be reduced.

3.5 Mechanics of laminate

3.5.1 The relation between stress-strain for the laminate

The representation of the mechanical behavior of the laminate is based on the micromechanics approach. Lamina's components (matrix and fibers) cannot be considered alone, but Lamina is taken as a whole. In the case of two laminae, the deformation must be an extended interface between the two laminas. The conditions that must be satisfied in two lamina with different orientations of fibers to form the laminate include deformation compatibility so that the lamina in the laminate deform along with the interface between that lamina in the direction of the applied force and the transverse stresses of lamina must be in equilibrium to correspond to the deformation. The problem becomes more complicated when the laminate contains more than two lamina in different orientations, necessitating a new approach known as the classical laminate theory, which is based on realistic assumptions that reduce the problem of

three-dimensional elasticity into two-dimensional with a review of the stress-strain behavior of lamina and application of the behavior to several of the Lamina in the laminate. The laminate thickness determines the stresses and strain changes.

The classical laminate theory assumes that the layers are a single laminate, perfectly connected. The laminate is thin, and the straight line perpendicular to the middle surface of the laminate remains a straight line and perpendicular to the middle surface after deformation. As figure 3.10 shows a section of the thin laminate before and after the deformation, This assumption leads to the transverse shear stress (τ_{xz} , τ_{yz}) in planes perpendicular to the middle surface of the laminate are zero, in addition to the shear strain (γ_{xz}, γ_{yz}) are zero [50].

The displacement of point C in the x-direction is

$$u = u_0 - z\beta \tag{3.65}$$

where u_0 is the displacement in the x-direction.

β is the slope of the middle surface laminate in the x-direction
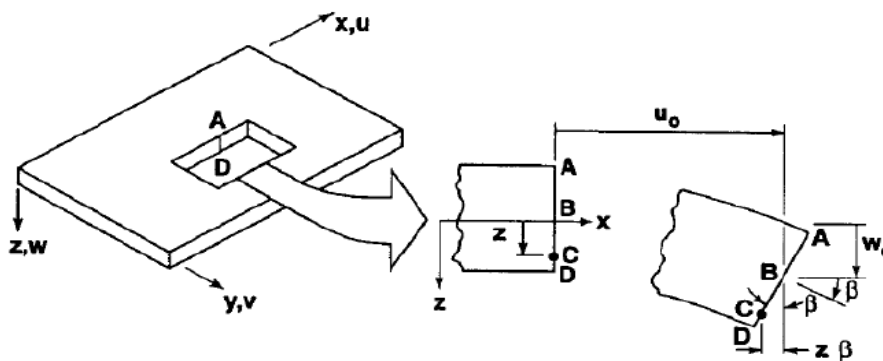
$$\beta = \frac{\partial w_0}{\partial x} \tag{3.66}$$

Figure 3.10 Deformation shape of the laminate in the plane [50].

$$u = u_0 - z\frac{\partial w_0}{\partial x} \tag{3.67}$$

Similarly, the displacement in the y-direction is

$$v = v_0 - z\frac{\partial w_0}{\partial y} \tag{3.68}$$

from the definition of the strain

$$\varepsilon_x = \frac{\partial u}{\partial x}, \; \varepsilon_y = \frac{\partial v}{\partial y}, \; \gamma_{xy} = \frac{\partial u}{\partial y} + \frac{\partial v}{\partial x}$$

$$\varepsilon_x = \frac{\partial u_0}{\partial x} - z\frac{\partial^2 w_0}{\partial x^2} \tag{3.69}$$

$$\varepsilon_y = \frac{\partial v_0}{\partial y} - z\frac{\partial^2 w_0}{\partial y^2} \tag{3.70}$$

$$\gamma_{xy} = \frac{\partial u_0}{\partial y} + \frac{\partial v_0}{\partial x} - z\frac{\partial^2 w_0}{\partial x \partial y} \tag{3.71}$$

The equations (69,70 and 71) can be written

$$\begin{bmatrix} \varepsilon_x \\ \varepsilon_y \\ \gamma_{xy} \end{bmatrix} = \begin{bmatrix} \frac{\partial u_0}{\partial x} \\ \frac{\partial v_0}{\partial y} \\ \frac{\partial u_0}{\partial y} + \frac{\partial v_0}{\partial x} \end{bmatrix} + z\begin{bmatrix} -\frac{\partial^2 w_0}{\partial x^2} \\ -\frac{\partial^2 w_0}{\partial y^2} \\ -2\frac{\partial^2 w_0}{\partial x \partial y} \end{bmatrix} = \begin{bmatrix} \varepsilon_x^0 \\ \varepsilon_y^0 \\ \gamma_{xy}^0 \end{bmatrix} + z\begin{bmatrix} k_x^0 \\ k_y^0 \\ k_{xy}^0 \end{bmatrix} \tag{3.72}$$

Where $\varepsilon_x^0, \varepsilon_y^0$ and γ_{xy}^0 are the three middle strains(elongations and distortion).

k_x^0, k_y^0 and k_{xy}^0 are the three middle surface curvatures (bending curvatures and torsion).

3.5.2 Strain and Stress in a Laminate

The global stresses for each lamina can be calculated from the stress-strain relationship in equation (3.62)[50].

$$\begin{bmatrix} \sigma_x \\ \sigma_y \\ \tau_{xy} \end{bmatrix} = \begin{bmatrix} \bar{Q}_{11} & \bar{Q}_{12} & \bar{Q}_{16} \\ \bar{Q}_{12} & \bar{Q}_{22} & \bar{Q}_{26} \\ \bar{Q}_{16} & \bar{Q}_{16} & \bar{Q}_{66} \end{bmatrix} \begin{bmatrix} \varepsilon_x^0 \\ \varepsilon_y^0 \\ \gamma_{xy}^0 \end{bmatrix} + z \begin{bmatrix} \bar{Q}_{11} & \bar{Q}_{12} & \bar{Q}_{16} \\ \bar{Q}_{12} & \bar{Q}_{22} & \bar{Q}_{26} \\ \bar{Q}_{16} & \bar{Q}_{16} & \bar{Q}_{66} \end{bmatrix} \begin{bmatrix} k_x^0 \\ k_y^0 \\ k_{xy}^0 \end{bmatrix} \quad (3.73)$$

The final stage of the classical laminate theory is the relationship between the forces and moments of the laminate with the strains and curvatures [50].
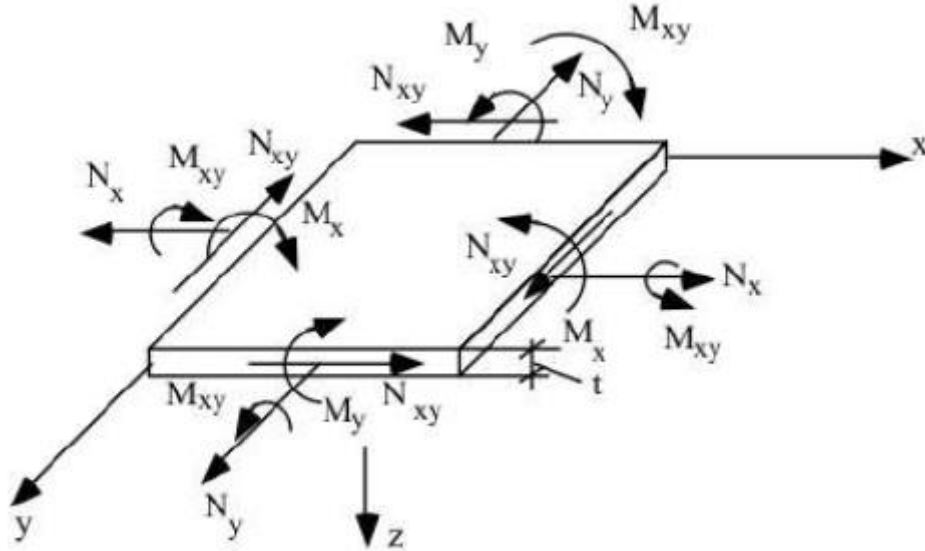
Figure 3.11 forces and moments of the laminate in the plane [50].

As in figure 3.11. The resultant forces and moments of the laminate are obtained by integrating the global stresses of each lamina through the thickness of the laminate.

$$N_x = \int_{-t/2}^{t/2} \sigma_x \, dz \ , \ N_y = \int_{-t/2}^{t/2} \sigma_y \, dz \ , \ N_{xy} = \int_{-t/2}^{t/2} \sigma_{xy} \, dz \quad (3.74)$$

$$M_x = \int_{-t/2}^{t/2} \sigma_x \, Z dz \ , \ M_y = \int_{-t/2}^{t/2} \sigma_y \, Z dz \ , \ M_{xy} = \int_{-t/2}^{t/2} \sigma_{xy} \, Z dz \quad (3.75)$$

Where t/2 is the half-thickness of laminate, as in figure 3.12.
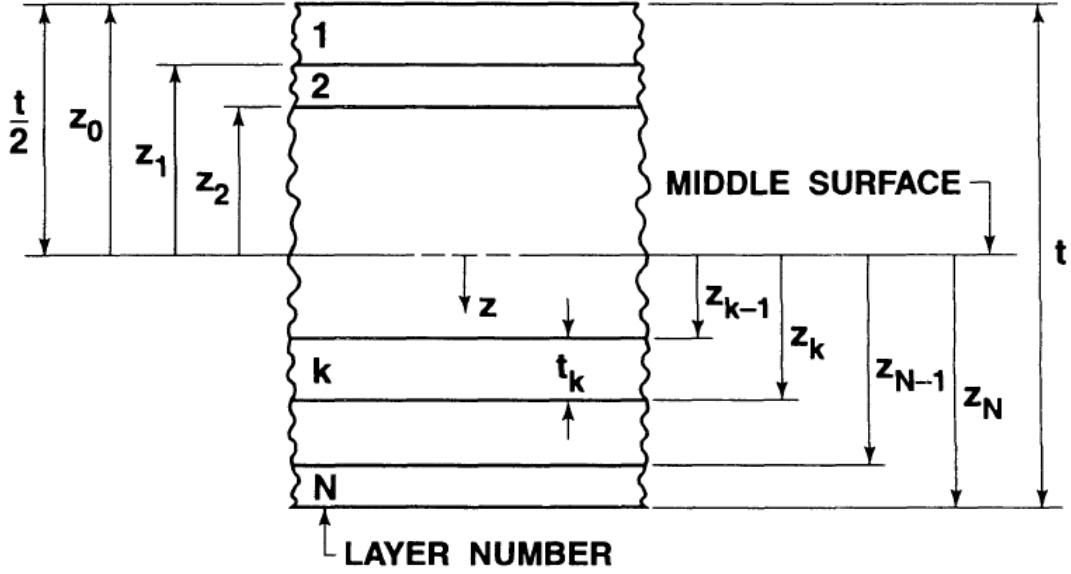
Figure 3.12 geometric shape of a laminate containing N of layers[50].

$$\begin{bmatrix} N_x \\ N_y \\ N_{xy} \end{bmatrix} = \sum_{k=1}^{n} \int_{z_{k-1}}^{z_k} \begin{bmatrix} \sigma_x \\ \sigma_y \\ \tau_{xy} \end{bmatrix} dz \tag{3.76}$$

$$\begin{bmatrix} M_x \\ M_y \\ M_{xy} \end{bmatrix} = \sum_{k=1}^{n} \int_{z_{k-1}}^{z_k} \begin{bmatrix} \sigma_x \\ \sigma_y \\ \tau_{xy} \end{bmatrix} Z dz \tag{3.77}$$

$$A_{ij} = \sum_{k=1}^{n} [\bar{Q}_{ij}]_k (z_k - z_{k-1}) \quad , i = 1,2,6 \ , j = 1,2,6 \tag{3.78}$$

$$B_{ij} = \frac{1}{2} \sum_{k=1}^{n} [\bar{Q}_{ij}]_k (z_k^2 - z_{k-1}^2) , i = 1,2,6 \ , j = 1,2,6 \tag{3.79}$$

$$D_{ij} = \frac{1}{3} \sum_{k=1}^{n} [\bar{Q}_{ij}]_k (z_K^3 - z_{K-1}^3) , i = 1,2,6 \ , j = 1,2,6 , \tag{3.80}$$

$$\begin{bmatrix} N_x \\ N_y \\ N_{xy} \end{bmatrix} = \begin{bmatrix} A_{11} & A_{12} & A_{16} \\ A_{12} & A_{22} & A_{26} \\ A_{16} & A_{26} & A_{66} \end{bmatrix} \begin{bmatrix} \varepsilon_x^0 \\ \varepsilon_y^0 \\ Y_{xy}^0 \end{bmatrix} + \begin{bmatrix} B_{11} & B_{12} & B_{16} \\ B_{12} & B_{22} & B_{26} \\ B_{16} & B_{26} & B_{66} \end{bmatrix} \begin{bmatrix} k_x \\ k_y \\ k_{xy} \end{bmatrix} \tag{3.81}$$

$$
\begin{bmatrix} M_x \\ M_y \\ M_{xy} \end{bmatrix} = \begin{bmatrix} B_{11} & B_{12} & B_{16} \\ B_{12} & B_{22} & B_{26} \\ B_{16} & B_{26} & B_{66} \end{bmatrix} \begin{bmatrix} \varepsilon_x^0 \\ \varepsilon_y^0 \\ \gamma_{xy}^0 \end{bmatrix} + \begin{bmatrix} D_{11} & D_{12} & D_{16} \\ D_{12} & D_{22} & D_{26} \\ D_{16} & D_{26} & D_{66} \end{bmatrix} \begin{bmatrix} k_x \\ k_y \\ k_{xy} \end{bmatrix}
\tag{3.82}
$$

Where

A_{ij} is an extensional stiffness matrix

B_{ij} is coupling stiffness matrix

D_{ij} is bending stiffness matrix

$$
\begin{bmatrix} N_X \\ N_y \\ N_{xy} \\ M_X \\ M_Y \\ M_{XY} \end{bmatrix} = \begin{bmatrix} A_{11} & A_{12} & A_{16} B_{11} & B_{12} & B_{16} \\ A_{12} & A_{22} & A_{26} B_{12} & B_{22} & B_{26} \\ A_{16} & A_{26} & A_{66} B_{16} & B_{26} & B_{66} \\ B_{11} & B_{12} & B_{16} D_{11} & D_{12} & D_{16} \\ B_{12} & B_{22} & B_{26} D_{12} & D_{22} & D_{26} \\ B_{16} & B_{26} & B_{66} D_{16} & D_{26} & D_{66} \end{bmatrix} \begin{bmatrix} \varepsilon_x^0 \\ \varepsilon_y^0 \\ \varepsilon_{Xy}^0 \\ k_x \\ k_y \\ k_{xy} \end{bmatrix}
\tag{3.83}
$$

3.6 Failure theories

3.6.1 Review of failure theories

Since the past four decades, the failure criteria for unidirectional composite materials have constantly evolved. The failure processes differ depending on the type of loading, the composite's components (fibers and matrix), and the bonding between them. The failure mechanisms have been thoroughly verified in a micromechanical and macro mechanical approach. It may be accurate to the commencement of Failure at critical locations of the Lamina and approximate to global Failure at the level of micromechanical behavior of the composite. However, the failure development of multi-directional laminate requires a macro-mechanical approach to determine the appropriate failure criterion [51].

Failure theories are built based on the parameters of strength and macroscopic stresses along the principal axes of the Lamina and the assumption of linear

elastic behavior of the Lamina. Failure theories are divided into three groups: the limited or non -interactive such as Maximum stress failure theory and Maximum strain failure theory, in which there is no interaction between the components of stress and components of the strain, interactive theories such as the theory of Tsai Hill failure theory and Tsai-Wu failure theory, which It is the opposite of the limited theories where there is an interaction between the components of stress and finally partial interaction theories or based on failure modes such as Hashin failure theory and puck failure theory [52].

3.6.2 The maximum stress failure theory.

This theory assumes that Failure occurs when any of the stresses on the local axes is equal to or exceeds the ultimate strength of CM [53]. It can be represented by three curves representing one of the failure modes, as in Figure 3.13.
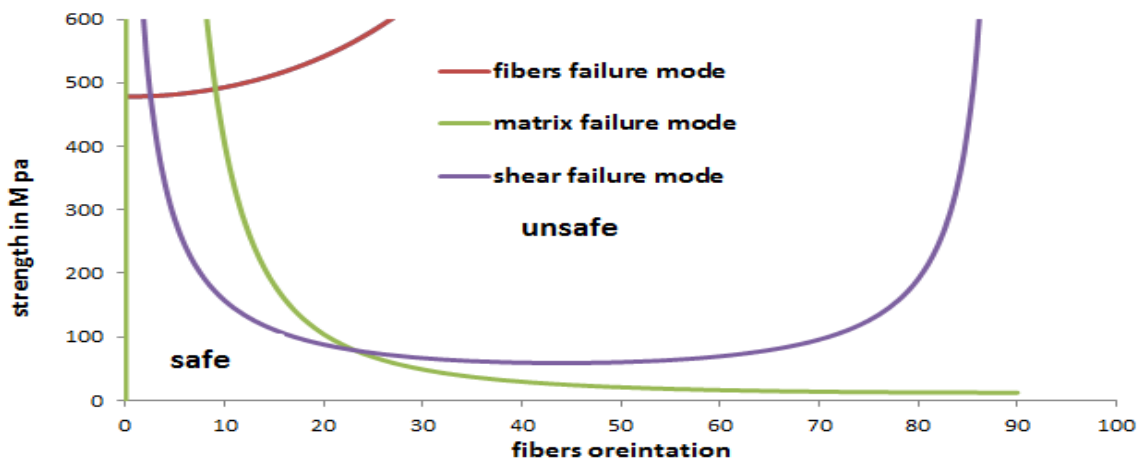

Figure 3.13 uniaxial strength of off-axis carbon/epoxy unidirectional Lamina (maximum stress theory)

Fibers failure mode $-(\sigma_1^C)_{ult} < \sigma_1 < (\sigma_1^T)_{ult}$ (3.84)

Matrix failure mode $-(\sigma_2^C)_{ult} < \sigma_2 < (\sigma_2^T)_{ult}$ (3.85)

Shear failure mode $-(\tau_{12})_{ult} < \tau_{12} < (\tau_{12})_{ult}$ (3.86)

3.6.3 The maximum strain failure theory.

This theory assumes that the Failure occurs if the strains (ε_1, ε_2, γ_{12})on local axes equal or exceed the ultimate strain or shear strain. There is little interaction between the strain components due to the Poisson's ratio [53].

$$-(\varepsilon_1^C)_{ult} < \varepsilon_1 < (\varepsilon_1^T)_{ult} \tag{3.87}$$

$$-(\varepsilon_2^C)_{ult} < \varepsilon_2 < (\varepsilon_2^T)_{ult} \tag{3.88}$$

$$-(\gamma_{12})_{ult} < \gamma_{12} < (\gamma_{12})_{ult} \tag{3.89}$$

3.6.4 Tsai-Hil failure theory

This theory is based on von Mises's distortion energy criterion applied to isotropic materials. The strain energy of the body consists of two parts: the dilation energy resulting from changes in the volume of the body and the distortion energy resulting from a change in the shape of the body. The Failure occurs when the energy is greater than the dilation energy. Hill relied on Von's criterion for producing distortion energy for anisotropic materials. Tsai adapted it is for the unidirectional lamina and that the Failure occurs when the Equation below is achieved [54].

$$\frac{\sigma_1^2}{(\sigma_1^T)_{ult}^2} - \frac{\sigma_1\sigma_2}{(\sigma_1^T)_{ult}^2} + \frac{\sigma_2^2}{(\sigma_2^T)_{ult}^2} + \frac{\tau_{12}^2}{(\tau_{12})_{ult}^2} = 1 \tag{3.90}$$

3.6.5 Tsai–Wu Failure Theory

The total strain energy of the Beltrami is considered the basis for constructing this theory. Tsai -Wu applied the failure theory to the lamina and assumed that the Failure would occur if the following Equation were achieved:

$$H_1\,\sigma_1 + H_2\,\sigma_2 + H_6\,\tau_{12} + H_{11}\,\sigma_1^2 + H_{22}\,\sigma_2^2 + H_{66}\,\tau_{12}^2 + 2\,H_{12}\,\sigma_1\,\sigma_2 < 1 \quad (3.91)$$

Using the five strength parameters of lamina can calculate the H1, H2, H6, H11, H22, and H66[54].

$$H_1 = \frac{1}{(\sigma_1^T)ult} - \frac{1}{(\sigma_1^C)ult}, \qquad H_{11} = \frac{1}{(\sigma_1^T)ult\,(\sigma_1^C)ult},$$

$$H_2 = \frac{1}{(\sigma_2^T)ult} - \frac{1}{(\sigma_2^C)ult}, \qquad H_{22} = \frac{1}{(\sigma_2^T)ult\,(\sigma_2^C)ult}, \tag{3.92}$$

$$\text{Where } H_6 = 0, \qquad H_{66} = \frac{1}{(\tau_{12})^2 ult}$$

Moreover, H_{12} can be found by Some practical suggestions:

$$H_{12} = - \frac{1}{2(\sigma_1^T)^2 ult}, \text{ per Tsai–Hill's failure theory} \tag{3.93}$$

$$H_{12} = - \frac{1}{2(\sigma_1^T)ult\,(\sigma_1^C)ult}, \text{ per Hoffman criterion} \tag{3.94}$$

$$H_{12} = - \frac{1}{2} \sqrt{\frac{1}{(\sigma_1^T)ult\,(\sigma_1^C)ult\,(\sigma_2^T)ult\,(\sigma_2^C)ult}}, \text{ per Mises–Hencky criterion} \tag{3.95}$$

3.6.6 Hashin failure theory

The Hashin criterion is widely used in structural applications and considers the fracture's physical phenomena. It separates the fibers failure mode and matrix failure mode by type of loading. Hashin's theory has four separate failure modes: [55].

Tensile fibers mode $\sigma_1 > 1$

$$\frac{\sigma_1^2}{(\sigma_1^T)_{ult}^2} + \frac{\tau_{12}^2}{(\tau_{12})_{ult}^2} = 1 \tag{3.96}$$

Compression fibers mode $\sigma_1 < 1$

$$- \frac{\sigma_1}{(\sigma_1^C)_{ult}} = 1 \tag{3.97}$$

Tensile matrix mode $\sigma_2 > 1$

$$\frac{\sigma_2^2}{\left(\sigma_2^T\right)_{ult}^2} + \frac{\tau_{12}^2}{(\tau_{12})_{ult}^2} = 1 \tag{3.98}$$

Compression matrix mode $\sigma_2 < 1$

$$\frac{\tau_{12}^2}{(\tau_{12})_{ult}^2} - \frac{\sigma_2}{(\sigma_2^C)_{ult}} = 1 \tag{3.99}$$

3.7 Fatigue

Fatigue can be defined as failure under variable or repeated load. Fatigue in composite materials is complicated compared to isotropic materials such as metals, where several factors are involved in determining the mechanisms of fatigue: type of reinforcement, type of matrix, environmental conditions (temperature or moisture content), and type of loading (cyclic frequency, and stress ratio). Failure occurs due to fatigue with gradual, invisible deterioration over the lifespan in metals. There is no reduction in stiffness. The damage increases with small and visible cracks that unite to form larger cracks that eventually fracture. As for composite materials, the matter becomes more complicated. Because of the multiple types of damage, such as matrix fracture, fiber fracture, discharge, removal of the interconnection between the matrix and fiber, and buckling.[56,57].

3.7.1 The (S-N) curve

The Wohler diagram or an S-N curve describes metals' fatigue state. It states that the strength of a material decreases with the repeated load as the number of load cycles increases and vice versa. The fatigue life of composite materials is described based on engineering the S-N curve and the fatigue life using an equation

Basquin's Equation, where the relationship between stress capacity (strain) and fatigue life is determined[58].

The Basquin Equation is

$$s = aN_f^b \qquad (3.100)$$

Where S is the fatigue stress, N_f is the number of cycles at Failure

(a and b) are the constants of materials.

The least-square method can find the constants (a and b), After making the power equation in a logarithmic law.

3.9 MATLAB program

Defending of last ply failure load, an algorithm was used with the following interties.

1. Find in the stiffness matrix as shown in Equation (3.58)
2. Enter the number of layers, and their angles, where (I) represents the first layer's angles, (J) represents the second layer's angles, (K) represents the third layer's angles, (N) represents the fourth layer's angles. The counter (M)indicates the fifth layer's angles. Depending on the counters, the location of layers is changed.
3. find The distance (thickness) of ply to the mid-plane (z_k)
4. Create conditions that prevent the angle of the fibers in the laminate from repeating.
5. Equation (3.63) was used to obtain the modified, reduced stiffness matrix for the five layers.
6. Using Equation(3.78), to calculate the extensional stiffness matrix for five layers.

7. Using Equation(3.79) to calculate the five-layer coupling stiffness matrix.

8. Using Equation (3.80) to calculate the five-layer bending stiffness matrix.

9. Using Equation (3.72), to calculate the global strain for five layers.

10. Equation (3.73) is used to calculate the global stress for five layers.

11. The equation (3.60) finds the calculation transformation matrix for five levels.

12. Equation (3.59) is used to calculate the local stress for five layers.

13. Using the mode failure theory, to calculate the stress ratio for five layers (Hashin theory)

14. The reducer stiffness matrix has zero if the layer has a minimum strength ratio.

15. By eliminating the minimum stress ratio of the layer, the procedures are repeated.

16. Finally, divide the stress ratio by the laminate thickness to determine the maximum allowed stress.

The above algorithm can be represented briefly by the flow chart as in Appendix (A).

Chapter Four
Experimental Work

Chapter four

Experimental work

4.1 Introduction

This chapter includes the experimental work, which was divided into three parts. The first part contains tensile tests of the lamina with different fiber orientations to determine the mechanical characteristics of it (strength and modulus of elasticity), the second part entails determining the laminate's mechanical characteristics, and the third part consists of a fatigue test of the laminate, as in the diagram figure below 4.1.
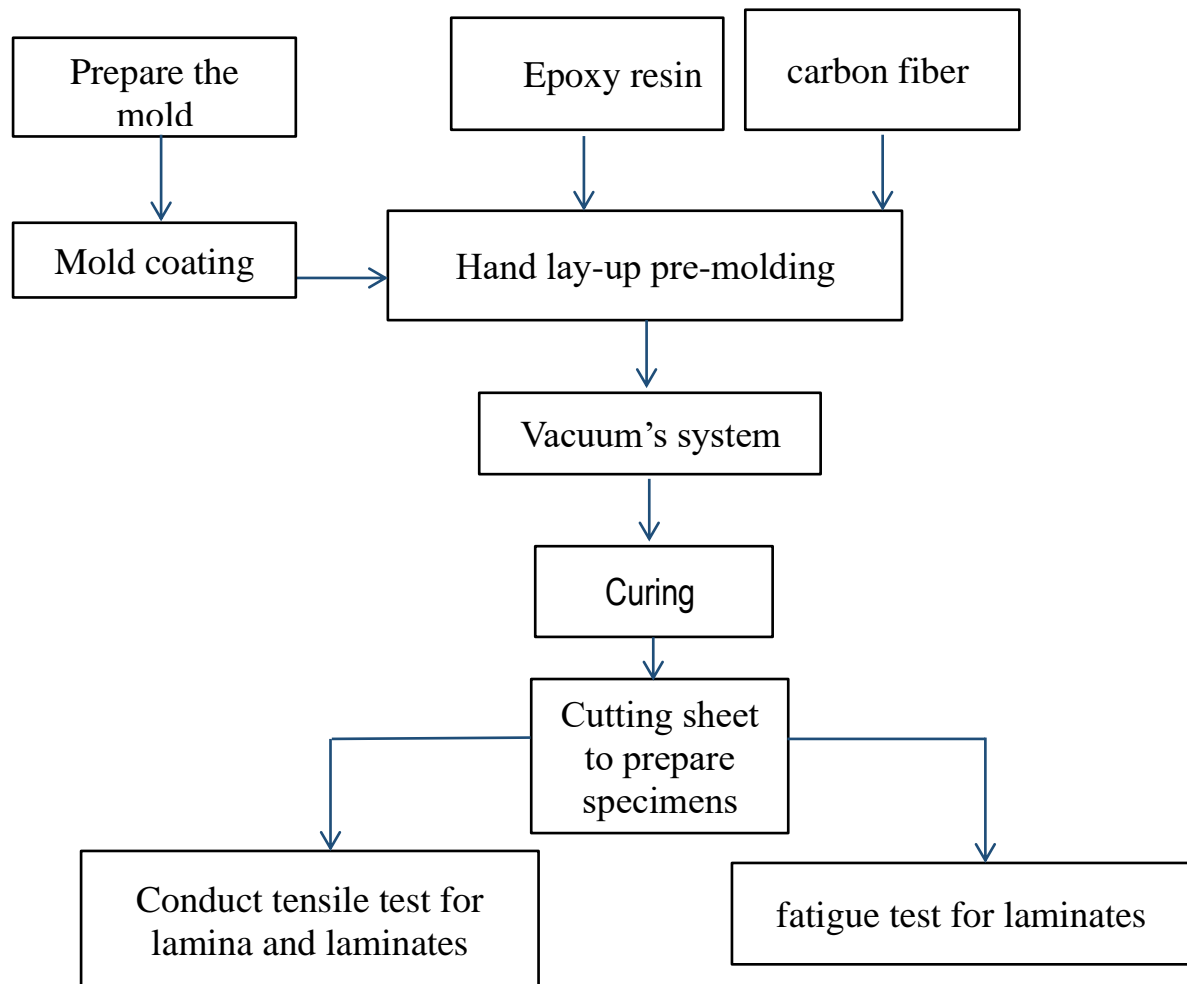
Figure 4.1 The diagram of experimental work.

4.2 Materials

The epoxy type (Quick mast 105 DCP) was used as a matrix for the composite material. It has low viscosity, low creep, good mechanical resistance, and can penetrate cracks up to 0.2 mm. Its properties are in table (4.1) [60].

Table (4.1) Mechanical Properties of epoxy [60].

Materials	Density (g/cm^3)	Tensile strength (MPa)	Compressive strength (MPa)	Young's modulus(GPa)	Poisson's ratio
Epoxy Quickmast-105	1.1	26	70	3.9	0.3

Unidirectional carbon fiber was used as reinforcement for epoxy and provided by from (Sika Wrap -300 Company, Switzerland) [61], as in the figure (4.2), and its properties in Table (4.2).

Table (4.2) physical and mechanical properties of carbon fibers [61].

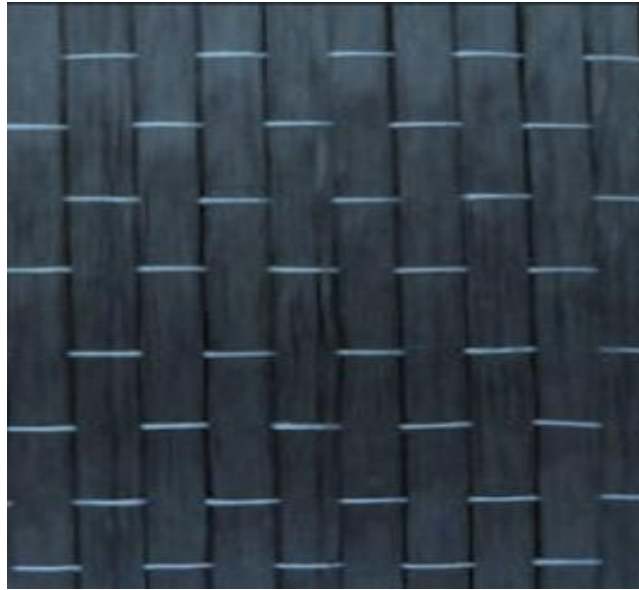| Materials	Density (g/cm^3)	Tensile strength (GPa)	Young's modulus(GPa)	Poisson's ratio
Carbon fibers	1.80	3.9	230	0.2

Figure 4.2: Unidirectional carbon fibers shape.

4.3 Fabricating Mold

The hand lay-up technique was used to make unidirectional laminates and laminates of unidirectional composite material with varied fiber angles simply and economically (0-90). A glass mold with (300x300x5)mm^3 was employed to achieve a flat surface, as shown in figure 4.3.
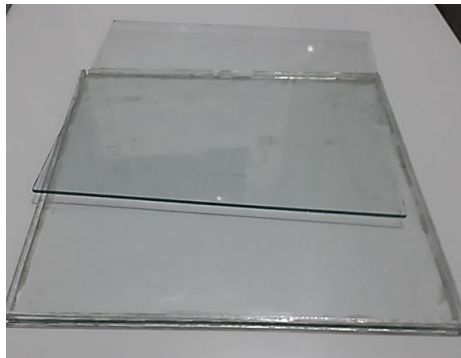

Figure 4.3 the shape of glass mold.

4.3.1 Manufacturing steps

1. Clean the mold and paint it with an oil gel to prevent the epoxy from sticking.

2. Preparing the epoxy according to the mixing ratio between the hardener and the base, with a ratio of 0.36%.

3. Cutting unidirectional carbon fibers according to the dimensions of the mold and the required fiber angle with a volume fraction of 30%.

4. Epoxy is placed in the mold to make a lamina, and then the fibers are placed over the epoxy. The brushes and Special rollers are used to wet the fibers and ensure their saturation with epoxy.

Figure 4.4 Manufacturing.

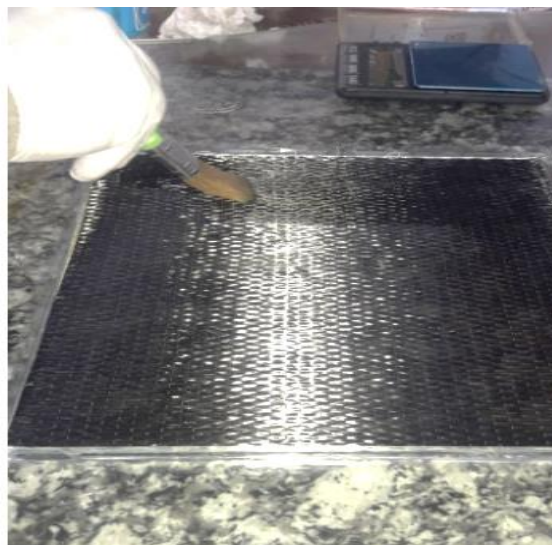5. To build a laminate consisting of five layers with different fibers angles by using the MATLAB program's outputs, Where step No. 4 is repeated with adding a layer of fibers and epoxy, and so on.

6. The vacuum system is used as in figure 4.5, where the mold is placed inside it for 24 hours and by pressure -1bar to get rid of air bubbles and preserve the volume fractions of the matrix and fibers.

Figure 4.5 Vacuum system.

7. Finally, the sheet is thermally treated by placing it in an oven at a temperature of 70ºC for three hours to obtain homogeneity and complete solidification.

8. The sheet is cut into samples according to the test required using a lathe machine (Suda ST1212 CNC router).

4.4 Tensile test

The tensile testing of the epoxy samples is carried out to obtain the required properties (ultimate stress, modulus of elasticity, and elongation at break). According to the standard ASTM D638 (2004) [62], as in figures 4.6 and 4.7. The tensile testing of carbon /epoxy samples is also carried out according to the standard ASTM D3039 [63] as in figures 4.8 and 4. 9 by using a tension machine (figure 4.10) (LARYEE-50 kN) with a strain rate (2mm/min) at room temperature, and three samples for each test, and take arranged value.
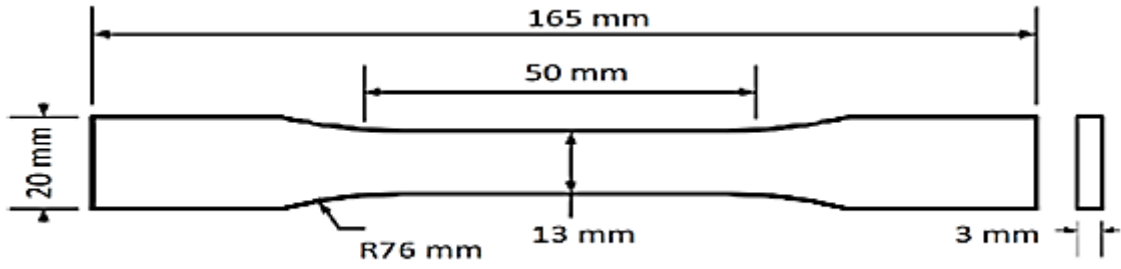
Figure 4.6 Scheme Shows the epoxy mold and dimension sample according to standard ASTM D638[62].

Figure 4.7 Epoxy sample.
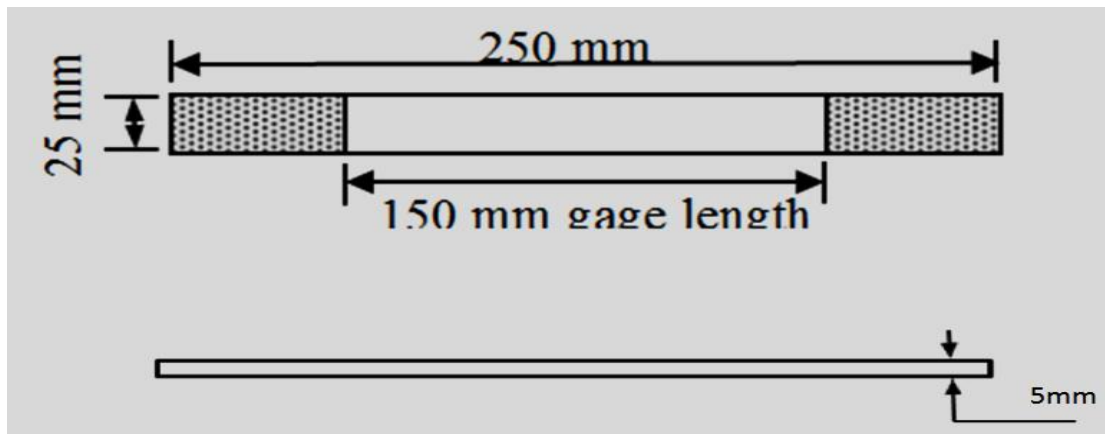
Figure 4.8 Diagram shows the sample's dimensions based on ASTM D3039 [63].
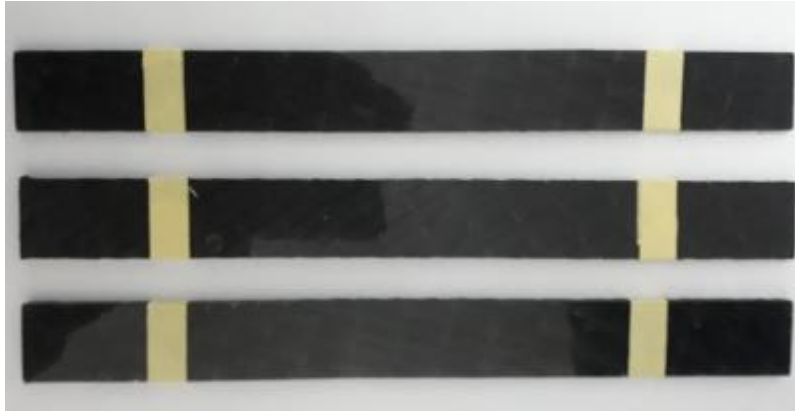
Figure 4.9 Samples are ready for testing.

Figure 4.10 tensile testing machine.

4.5 Fatigue test

A fatigue test was carried out for the laminate with five-layer (carbon /EP), where the samples were cut according to the fatigue testing machine, as shown in Figures 4.11 and 4.12. The fatigue test was conducted by alternating full

reverse bending the testing machine HSM20 as in Figure 4.13[64] using seven samples to find the S-N curve for each laminate. The device works at a speed of 1400 rpm, a voltage of 230v, and a frequency of 20 Hz. The test was Carried out at room temperature and a stress ratio (R=-1).
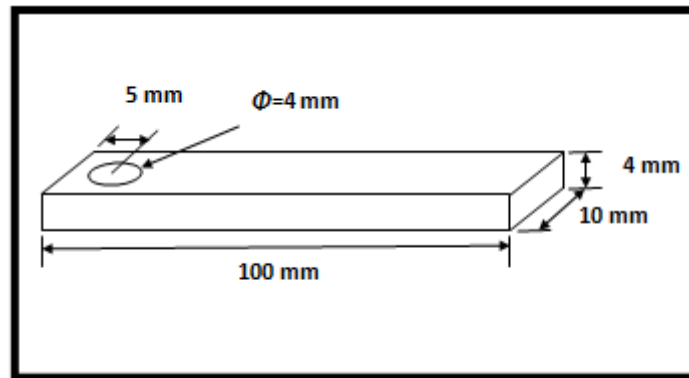
Figure 4.11Schematic specimens of fatigue test[64].

Figure 4.12 Sample dimensions of fatigue test.

Figure 4.13 the testing machine (HSM20) of fatigue.

Chapter Five
Results and Discussion

Results and Discussion

5.4 Introduction

This chapter includes three parts to discuss the theoretical and experimental results accurately and scientifically. The first part had the theoretical results obtained using micro-mechanics analysis, which relies on the properties of the Lamina's components (matrix and fibers) to draw the curves of common failure theories and compare them to the experimental results to select the most appropriate theory. The experimental results included conducting a tensile test of Lamina's samples with different fiber angles (0° to 90°).

The second part includes the theoretical results to obtain different sequences in 72 different sequences of the laminates for five layers using the Mat lab program (R2018) compared with the experimental results. Finally, the third part included a fatigue test for three different laminate sequences and a scanning electron microscope (SEM) test for the fracture region.

5.2 Tensile strength of lamina

5.2.1 Theoretical tensile strength of lamina.

The stiffness and strength parameters were calculated based on the micromechanics approach of CM as in table (5.1); the tensile strength for off-axis laminas was calculated based on the criteria of each theory, and the theoretical tensile strength was found based on the criterion of each theory.

Table (5.1) The parameters stiffness and strength of unidirectional
Lamina (carbon/epoxy).

No	Parameters stiffness and strength	The value
1	Longitudinal modulus of CM	71.23GPa
2	Transverse modulus of CM	5.56 GPa
3	Major poison's ratio of CM	0.305
4	Shear modulus of CM	2.054GPa
5	Ultimate longitudinal tensile strength	478.2MPa
6	Ultimate longitudinal compression strength	63.5MPa
7	Ultimate transverse tensile strength	12.204MPa
8	Ultimate transverse compression strength	26.73MPa
9	Ultimate shear strength	29.47MPa

The theoretical results showed that the tensile strength decreases with increasing the angle of the fibers, as shown in figure 5.1. Simultaneously, the curves of theories approach each other when the angle of fiber orientations for the lamina is increased due to the appearance of the tensile effect in the matrix in addition to the shear between the matrix and the fibers. This can be seen in the maximum stress failure theory.
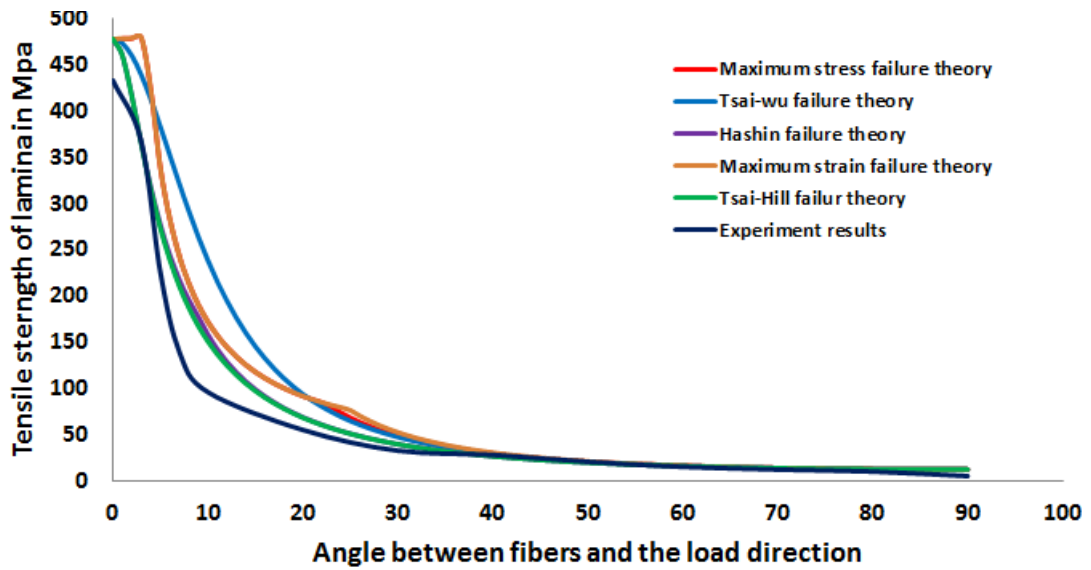
Figure 5.1failure criteria curves for carbon/epoxy with different angles fibers.

There was a congruence between the Maximum stress failure theory and the Maximum strain failure theory. The effect of the Poisson's ratio was clear, as in figure 5.2 between($26^{°}$-$35°$) of fibers angles.
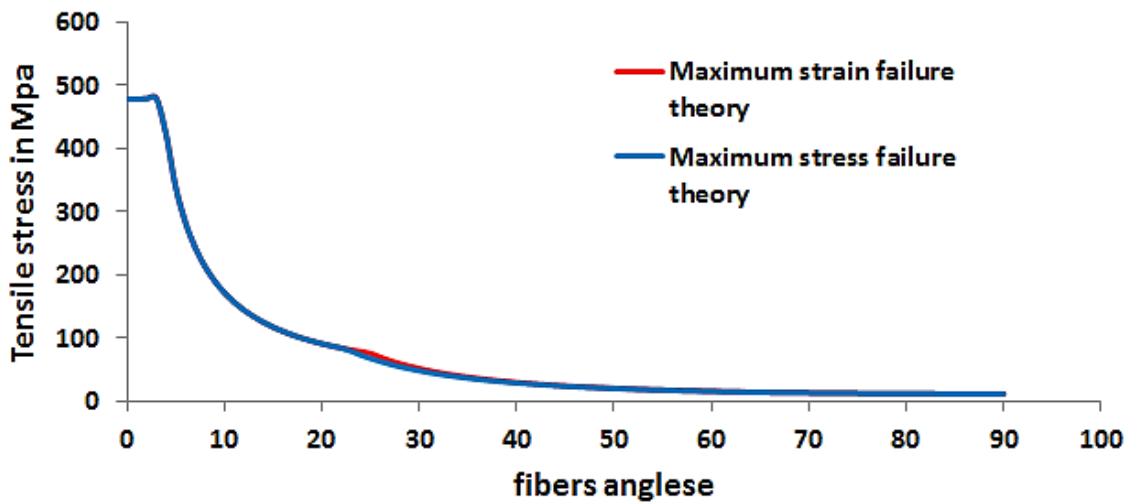
Figure 5.2 shows the difference between the maximum stress and maximum strain criteria.

In the figure (5.3), the effect of the element H_{12} in the Tsai-Wu criterion has been neglected, as there is a match with most of the empirical formulas and that its effect is very small and does not affect the results of the theory [50].
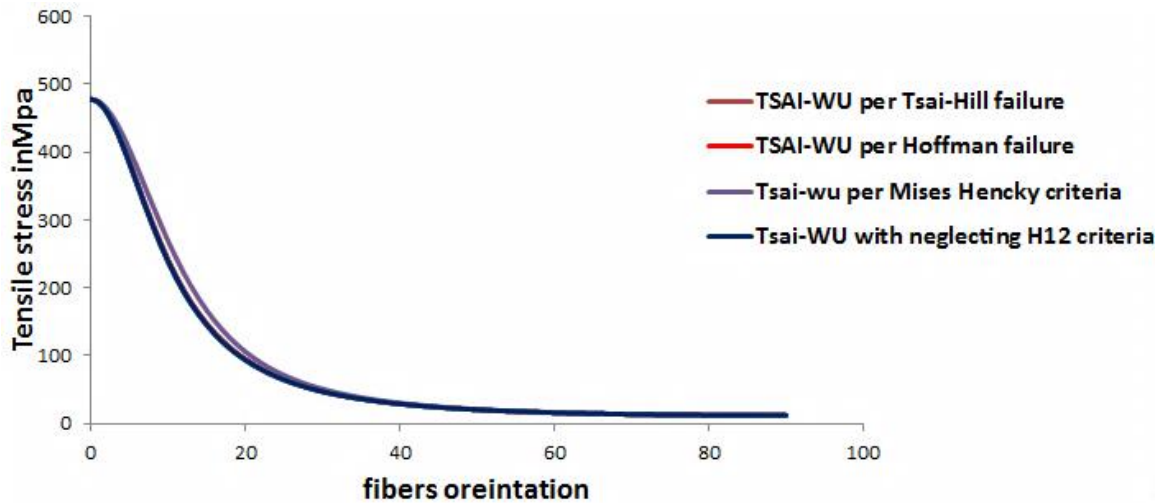
Figure 5.3 Sketch of Tsai-Wu theory with empirical hypotheses for an element H_{12}.

5.2.2 Experimental tensile strength of lamina

The tensile test was carried out on 13 samples of unidirectional laminas with different fibers angles from (0°-90°) as in table (5.2), where it was noticed that the uniaxial load is decreased with the increase in the direction angle of fibers, and these results are consistent with reference [20].

Table (5.2) Experimental tensile strength of lamina (carbon/epoxy).

Number of specimens	Specimen with angle fibers orientation in degree	Tensile strength in (Mpa)
1	0	430.35
2	3	361.346
3	5	226.045
4	7	139.527
5	10	96.289
6	20	55.853
7	30	32.573
8	40	27.966
9	50	20.648
10	60	15.125
11	70	12.063
12	80	9.926
13	90	5.078

Figures 5.4 and 5.5 show the relationship of stress with strain, where the elastic behavior of the CM appears at a slight angle for fibers. The elastic behavior reduces as the angle of the direction of the fibers increases because the uniaxial load tilts away from the direction of the fibers, resulting in the appearance of the matrix effect. This conclusion accords with reference [49] in that the shear force between the fibers and the matrix emerges, causing a fracture. This explains the occurrence of the fracture towards the angle of the fibers, as in figure 5.6.
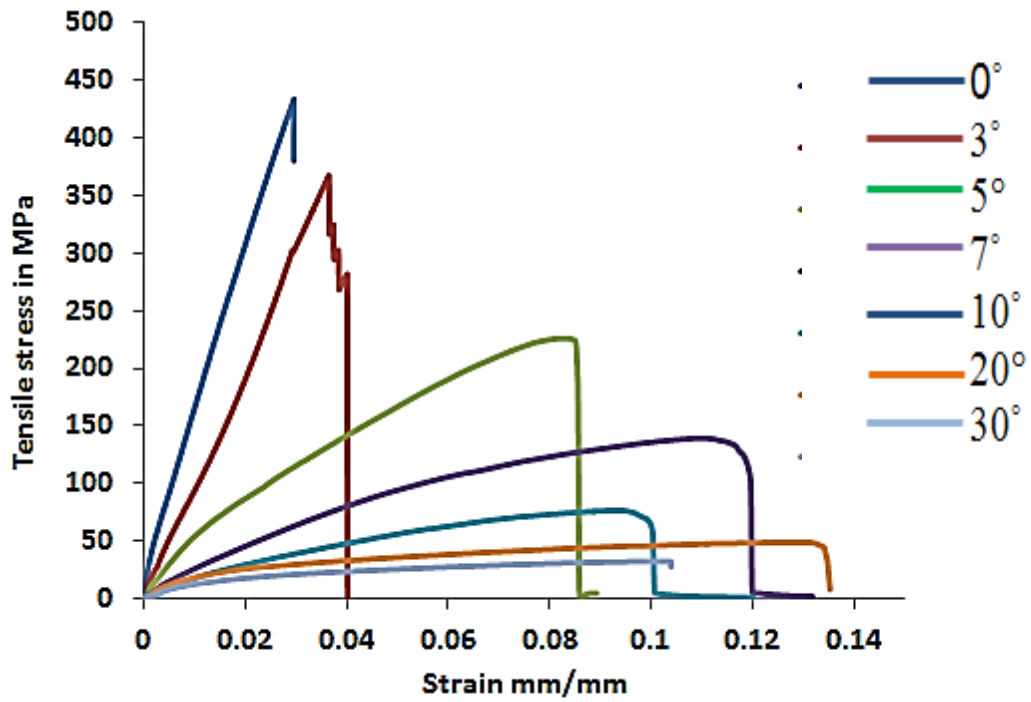
Figure 5.4 stress-strain curves of carbon/epoxy with fibers orientation (0,3,5,7,10,20,30).
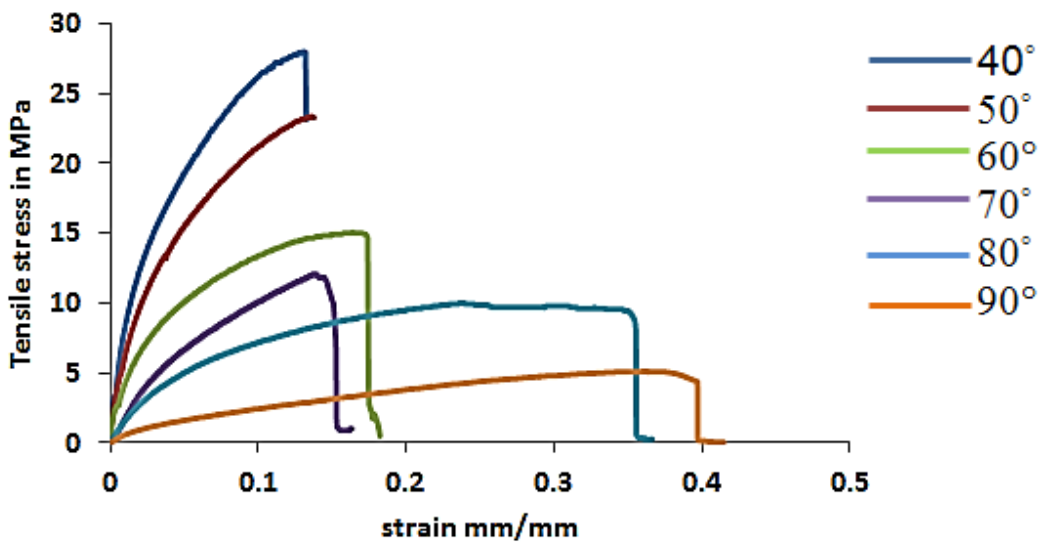
Figure 5.5 stress-strain curves of carbon/epoxy with fibers orientation (40,50,60,70,80,90).

Figure 5.6 the fracture in the lamina (carbon/epoxy) with different fibers
Orientation.

5.2.3 Comparison of theoretical and experimental results

A comparison was made between the experimental results obtained from the tensile test with the theoretical results of the theories of failure. As indicated in figure 5.7, Hashin's theory had the greatest acceptability, followed by Tsai-Hill's approach, which had good acceptability. In contrast, the rest of the ideas came successively, and the Tsai-Wu theory was the farthest from the practical results.
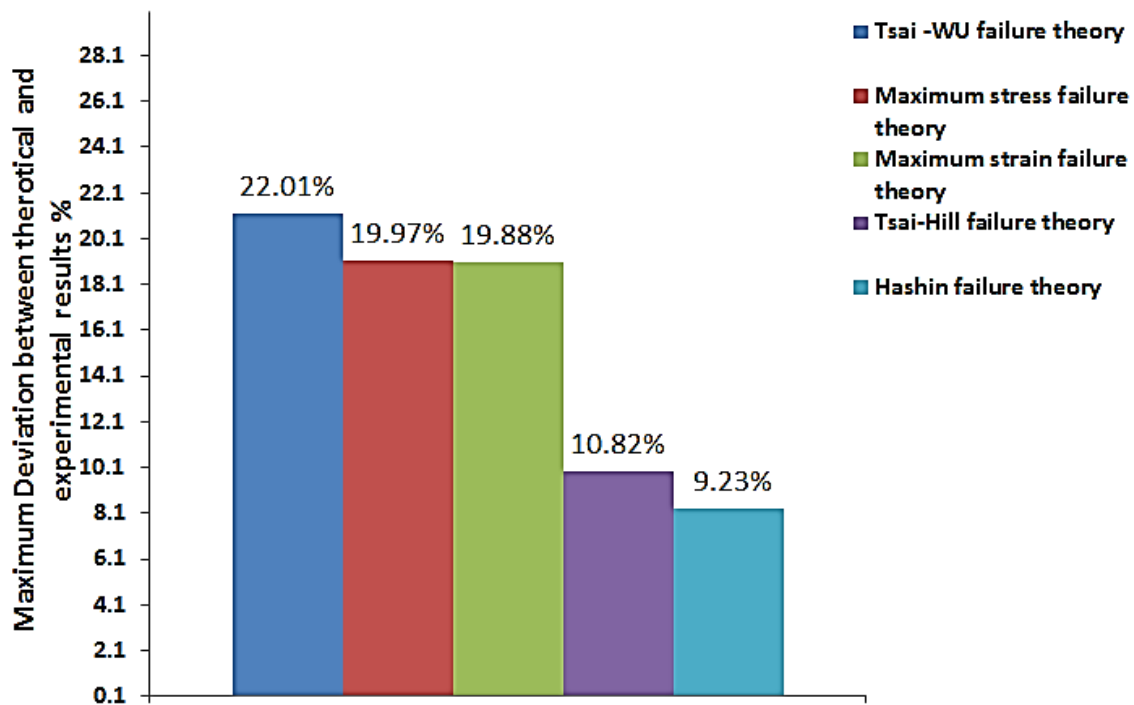
Figure 5.7 the percentage of the mean deviation between the results of failure theories and the experimental results.

Two patterns participated in drawing Hashin's theory, which is the mode of fibers failure and the mode of matrix failure under the influence of tensile load. Figure 5.8 shows good convergence with the experimental results. Also, Tsai Hill's theory showed good acceptance with experimental effects, and this finding agrees with reference [20].
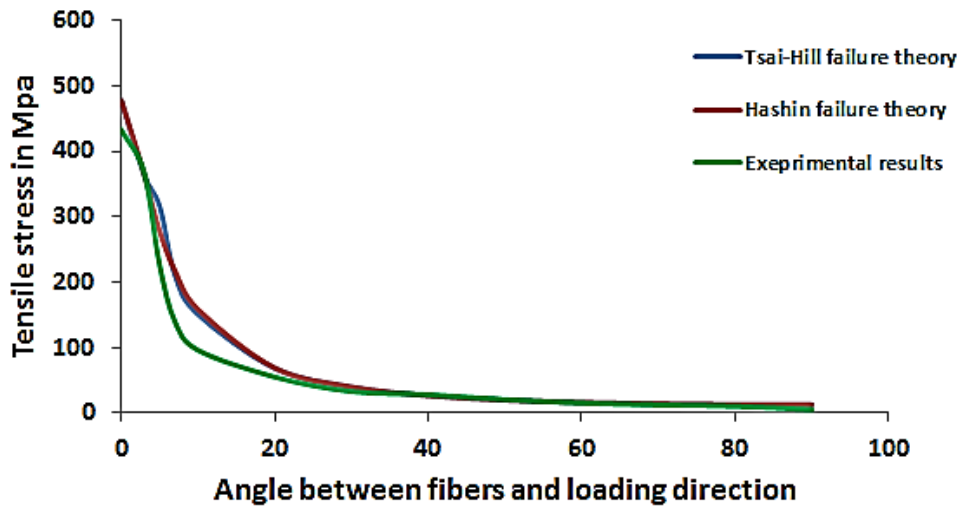
Figure 5.8 a comparison between the results of the theories of Hashin and Tsai-Hill and the experimental results.

5.3 Tensile strength of the laminate

5.3.1 Theoretical tensile strength of the laminate

Different stacking sequences of the laminates were created as indicated in tables 5.3, 5.4, 5.5, 5.6, and 5.7 depending on the characteristics of the Lamina (carbon/EP) by applying the elasticity laws of CM and CLT with the assistance of the Matlab software, as described in the introduction to this chapter.

Various laminate stacking sequences of up to 120 laminates with sixty tensile stress values were obtained due to the similarity between laminates.

It was observed. that the group of laminates that begins with a layer having a fiber direction (0°) has low tensile strength values as table 5.3 compared to the rest of the laminates, where the tensile stress values range from 48.228Mpa to 29.437Mpa.

Table (5.3) The theoretical results of tensile stress for the group of laminate which begins with a layer that has fibers direction (0°)

No of laminate	Stacking sequence of laminate	Tensile stress (MPa)	No of laminate	Stacking sequence of laminate	Tensile stress (MPa)
1	[0/30/60/90/75]	30.107	13	[0/30/60/75/90]	31.363
2	[0/30/90/60/75]	29.748	14	[0/30/90/75/60]	30.166
3	[0/60/30/90/75]	43.212	15	[0/60/30/75/90]	44.741
4	[0/60/90/30/75]	40.658	16	[0/60/90/75/30]	42.084
5	[0/90/30/60/75]	37.602	17	[0/90/30/75/60]	36.739
6	[0/90/60/30/75]	37.555	18	[0/90/60/75/30]	37.431
7	[0/75/30/60/90]	48.228	19	[0/30/75/60/90]	29.437
8	[0/75/30/90/60]	44.573	20	[0/30/75/90/60]	29.437
9	[0/75/60/30/90]	46.036	21	[0/60/75/30/90]	45.731
10	[0/75/60/90/30]	43.810	22	[0/60/75/90/30]	44.734
11	[0/75/90/30/60]	37.777	23	[0/90/75/30/60]	32.950
12	[0/75/90/60/30]	39.762	24	[0/90/75/60/30]	35.201

As shown in table 5.4, the second laminate group starts with a layer having a 30° fiber orientation, where the stress values range from 150.270MPa to 33. 734MPa. This group had better stresses values than the laminate of the first group.

Table (5.4) The theoretical results of tensile stress for the group of laminate which begins with a layer that has fibers direction (30°)

No of laminate	Stacking sequence of laminate	Tensile stress (MPa)	No of laminate	Stacking sequence of laminate	Tensile stress (MPa)
1	[30/0/60/90/75]	37.839	13	[30/0/75/60/90]	35.585
2	[30/0/90/60/75]	33.734	14	[30/0/75/90/60]	35.103
3	[30/60/0/90/75]	147.770	15	[30/60/75/0/90]	51.749
4	[30/60/90/0/75]	58.256	16	[30/60/75/90/0]	35.201
5	[30/90/0/60/75]	138.370	17	[30/90/75/0/60]	67.841
6	[30/90/60/0/75]	66.345	18	[30/90/75/60/0]	44.734
7	[30/75/0/60/90]	150.270	19	[30/0/60/75/90]	39.573
8	[30/75/0/90/60]	149.480	20	[30/0/90/75/60]	34.227
9	[30/75/60/0/90]	54.195	21	[30/60/0/75/90]	140.890
10	[30/75/60/90/0]	37.431	22	[30/60/90/75/0]	39.762
11	[30/75/90/0/60]	60.458	23	[30/90/0/75/60]	138.670
12	[30/75/90/60/0]	42.084	24	[30/90/60/75/0]	43.810

The third group of laminates begins with a layer having a direction of fibers 60, where the stress values ranged from 160.890 MPa to 29.743MPa Some of its laminates have obtained the highest tensile stress.

Table (5.5) The theoretical results of tensile stress for the group of laminate which begins with a layer that has fibers direction (60°)

No of laminate	Stacking sequence of laminate	Tensile stress (MPa)	No of laminate	Stacking sequence of laminate	Tensile stress (MPa)
1	[60/0/30/60/75]	56.125	13	[60/0/75/30/90]	63.276
2	[60/0/60/30/75]	52.703	14	[60/0/75/90/30]	67.841
3	[60/30/0/90/75]	160.890	15	[60/30/75/0/90]	44.498
4	[60/30/90/0/75]	50.253	16	[60/30/75/90/0]	32.950
5	[60/90/0/30/75]	160.520	17	[60/90/75/0/30]	35.103
6	[60/90/30/0/75]	51.556	18	[60/90/75/30/0]	29.473
7	[60/75/0/30/90]	133.630	19	[60/0/30/75/90]	58.578
8	[60/75/0/90/30]	138.670	20	[60/0/90/75/30]	60.458
9	[60/75/30/0/90]	49.206	21	[60/30/0/75/90]	151.880
10	[60/75/30/90/0]	36.739	22	[60/30/90/75/0]	37.777
11	[60/75/90/0/30]	34.227	23	[60/90/0/75/30]	149.480
12	[60/75/90/30/0]	30.166	24	[60/90/30/75/0]	44.573

As shown in tables 5.6 and 5.7, the stacking sequence of laminates that begin with a layer is 90 degrees, and the stacking sequence of laminates that start with a layer is 75 degrees. In terms of behavior and the influence of fiber orientation on strength, they are similar to the other categories. The laminate sequences in which a layer has the orientation of the fibers 0, positioned in the center of the laminate. They have the highest stress.

Table (5.6) The theoretical results of tensile stress for the group of laminate which begins with a layer that has fibers direction (90°)

No of laminate	Stacking sequence of laminate	Tensile stress (Mpa)	No of laminate	Stacking sequence of laminate	Tensile stress (Mpa)
1	[90/0/30/60/75]	47.048	13	[90/0/75/30/60]	44.498
2	[90/0/60/30/75]	49.063	14	[90/0/75/60/30]	51.749
3	[90/30/0/60/75]	131.690	15	[90/30/75/0/60]	63.276
4	[90/30/60/0/75]	63.421	16	[90/30/75/60/0]	45.731
5	[90/60/0/30/75]	158.69	17	[90/60/75/0/30]	35.585
6	[90/60/30/0/75]	55.526	18	[90/60/75/30/0]	29.437
7	[90/75/0/30/60]	151.88	19	[90/0/30/75/60]	49.206
8	[90/75/0/60/30]	140.89	20	[90/0/60/75/30]	54.195
9	[90/75/30/0/60]	58.578	21	[90/30/0/75/60]	133.630
10	[90/75/30/60/0]	44.741	22	[90/30/60/75/0]	46.036
11	[90/75/60/0/30]	39.573	23	[90/60/0/75/30]	150.270
12	[90/75/60/30/0]	31.363	24	[90/60/30/75/0]	48.224

Table (5.7) The theoretical results of tensile stress for the group of laminate which begins with a layer that has fibers direction (75°)

No of laminate	Stacking sequence of laminate	Tensile stress (Mpa)	No of laminate	Stacking sequence of laminate	Tensile stress (Mpa)
1	[75/0/30/60/90]	55.526	13	[75/60/0/30/90]	131.690
2	[75/0/30/90/60]	51.556	14	[75/60/0/90/30]	138.370
3	[75/0/60/30/90]	63.421	15	[75/60/30/0/90]	47.048
4	[75/0/60/90/30]	66.345	16	[75/60/30/90/0]	37.602
5	[75/0/90/30/60]]	50.253	17	[75/60/90/0/30]	33.734
6	[75/0/90/60/30]	58.256	18	[75/60/90/30/0]	29.748
7	[75/30/0/60/90]	158.69	19	[75/90/0/30/60]	160.890
8	[75/30/0/90/60]	160.520	20	[75/90/0/60/30]	147.777
9	[75/30/60/0/90]	49.063	21	[75/90/30/0/60]	56.125
10	[75/30/60/90/0]	37.555	22	[75/90/30/60/0]	43.212
11	[75/30/90/0/60]	52.703	23	[75/90/60/0/30]	37.839
12	[75/30/90/60/0]	40.658	24	[75/90/60/30/0]	30.107

A laminate will fail under increasing mechanical loads until failing occurs in the last ply. The laminate failure, however, may not be catastrophic. It is possible that some layer fails first and that the composite continues to take more loads until all the plies fail. Failed plies may still contribute to the stiffness and strength of the laminate if their fibers are still not failed while their matrices are cracked along the fibers. Even if that occurs, each failed ply will lose its strength and trend dramatically to complete failure (i.e. its fibers will fail too).

When a ply fails, it may have cracks parallel to the fibers. This ply is still capable of taking load parallel to the fibers. Here, the cracked ply can be replaced by a hypothetical ply that has no transverse stiffness, transverse tensile

strength, and shear strength. The longitudinal modulus and strength remain unchanged. When a ply fails, fully discount the ply and replace the ply of near zero stiffness and strength. In this case, there will be an eccentric between the applied axial tensile force and the neutral axis of the overall remaining plies. Hence, there will be a bending moment caused by this eccentricity in addition to the axial load. The resulted stresses will be combined stresses which are direct and flexural stresses.

Increasing the eccentricity after the failure of the first ply will lead to increasing the resulting combined stresses and hence, diminishing the strength of the laminates. This was very clear in our results since the laminates that containing plies with (0° fibers orientations) at one of their edges, provide the worsen strength. On the other hands, all laminates that have (0° oriented plies) at their centers provides highest strength against the tensile loads.

As a result, it can be noted that the presence of eccentricity between the applied axial loads and the neutral axis of the overall plies will highly affect the laminated strength. Hence, the plies sequences within laminates are an important parameter and highly affected the experimental results.

5.3.2 Experimental tensile test

Three laminates of different stresses were taken, where the laminate [60/30/0/90/75] represented the highest theoretical stress, the laminate [30/90/0/60/75] represented the middle value of the stress and the laminate [0/30/60/90/75] represented the lowest stress. A tensile test was performed on the three laminates in Figure 5.9. The experimental results showed that the tensile properties depend mainly on the direction, strength of the fibers and the sequence of layers. The first and second sequences laminates had a higher tensile stress value than the third laminate because the layer with zero fiber direction is located in the middle of the laminate, which may be the reason for

obtaining good values tensile stress. The tensile stresses of the laminates
([60/30/0/90/75] ,

[30/90/0/60/75],and[0/30/60/90/75]) were 150.202MPa

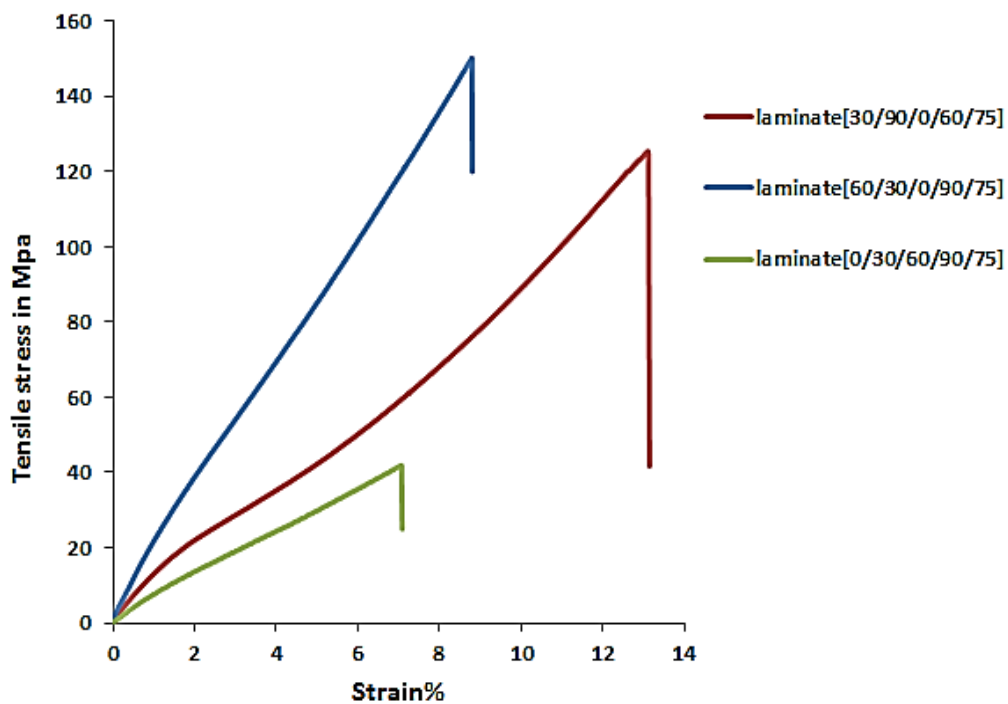125.436MPa, and 41.124MPa, respectively.

.

Figure 5.9 stress-strain for three laminates (laminate [60/30/0/90/75]
,laminate[30/90/0/60/75] and laminate[0/30/60/90/75]).

5.3.3 Comparing experimental and theoretical results for tensile stress of laminate.

Table 5.8 shows the theoretical and experimental results. There was good acceptability of the results. The stress of the laminates was affected by the sequence of layers and the direction of the fibers. The laminate [60/30/0/90/75] obtained the highest stress value, while the laminate [0/30/60/90/75] was expected to be the lowest. The value of the deviation is good between the results except for the laminate [0/30/60/90/75], which recorded a significant deviation compared to the other two laminates.

Table (5.8) Comparison between theoretical and Experimental results

NO.	Laminate	Theoretical tension strength(MPa)	Experimental tension strength(MPa)	Different ratio %
1	[60/30/090/75]	160.890	150.202	6.64%
2	[30/90/0/60/75]	138.370	125.436	9.34%
3	[0/30/60/90/75]	30.107	41.124	27%

5.4 Fatigue test for laminates

The fatigue test was conducted on three laminates of different sequences, with 21 samples for each laminate, seven samples with constant amplitude loading as a fully reversed (stress ratio R= -1) to determine S-N curves. Where fatigue curves were obtained using an angle suitable for the experimental results. Table 5.9 shows the results of the power equation (Basquin's equation) for the experimental results. Where a and b are the equation's constant and curve exponent, respectively, and both define the composite material's fatigue behavior. R2 represents the correlation factor, and curves with a high correlation lead to well-explained experimental data in the power equation. The fatigue limit of composite materials is considered so that the fatigue life becomes infinite when the material exceeds several cycles up to 10^6 [64].In

general, the fatigue strength is directly proportional to the ultimate tensile strength[65].

Table (5.9) Power equation coefficients to calculate fatigue life

laminate	a	b	R²
[60/30/0/90/75]	925.1	-0.188	0.942
[30/90/0/60/75]	635.66	-0.178	0.952
[0/30/60/90/75]	698.2	-0.278	0.944

In Figure 5.10, it is observed that the laminate [60/30/0/90/75] and the laminate [30/90/0/60/75] had reached their fatigue limit after the fatigue strength had reached 0.4 of ultimate tensile stress. In contrast, the laminate [0/30/60/90/75] has reached the fatigue limit after the fatigue strength has reached 0.3 of UTS.

This indicates the effect of the direction of the fibers and the sequence of layers on the fatigue life.
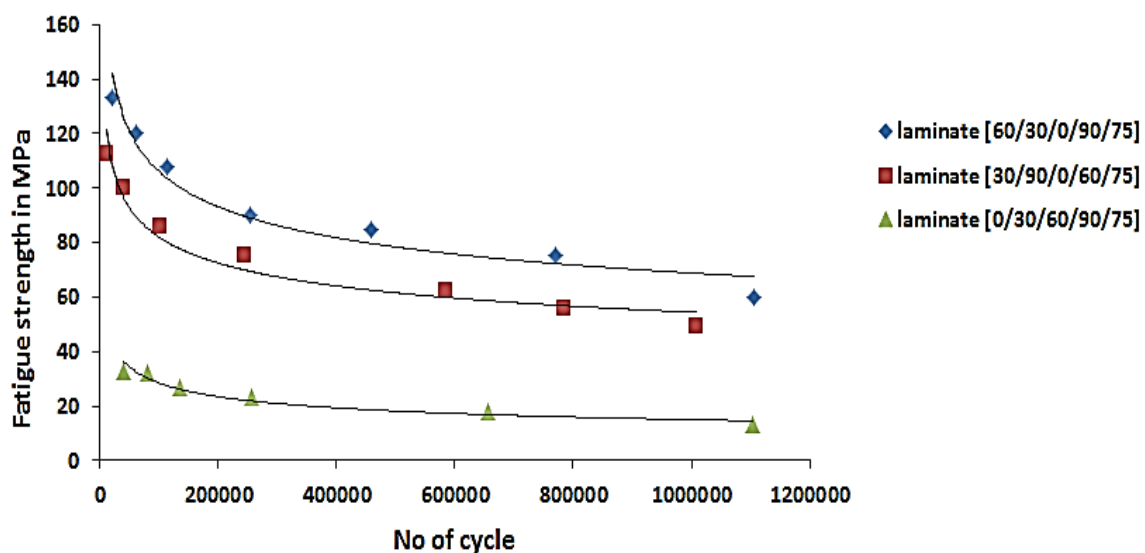

Figure 5.10 the S-N curves of carbon/epoxy with different laminates.

5.5 Scanning electron microscope

 A scanning electron microscope was used to examine the fracture region due to fully reversed flexural fatigue to investigate the microstructure of specimens. Figure 5.11 shows the failure patterns of the laminate [0/30/60/90/75], where the fiber fracture and the matrix and delamination between the layers are apparent, and the crack expansion was significant compared to the other laminates. Figure 5.12 represented the laminate [60/30/0/90/75]. Likewise, the fracture region of fibers and matrix was transparent, and the interconnection between them, but the cracks related to the delamination were smallest compared to other laminates.

The fibers and matrix breakdown were visible in the last figure 5.13 for The laminate [30/90/0/60/75], similar to its predecessors. Despite this, a transverse crack occurred in the fracture location, indicating that the layer was weak, allowing the cracks to form.

a
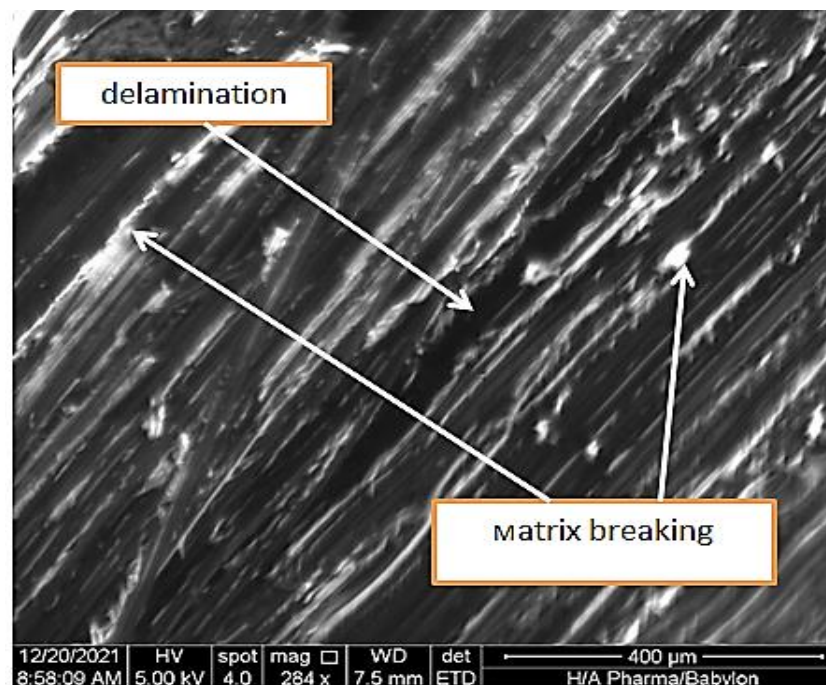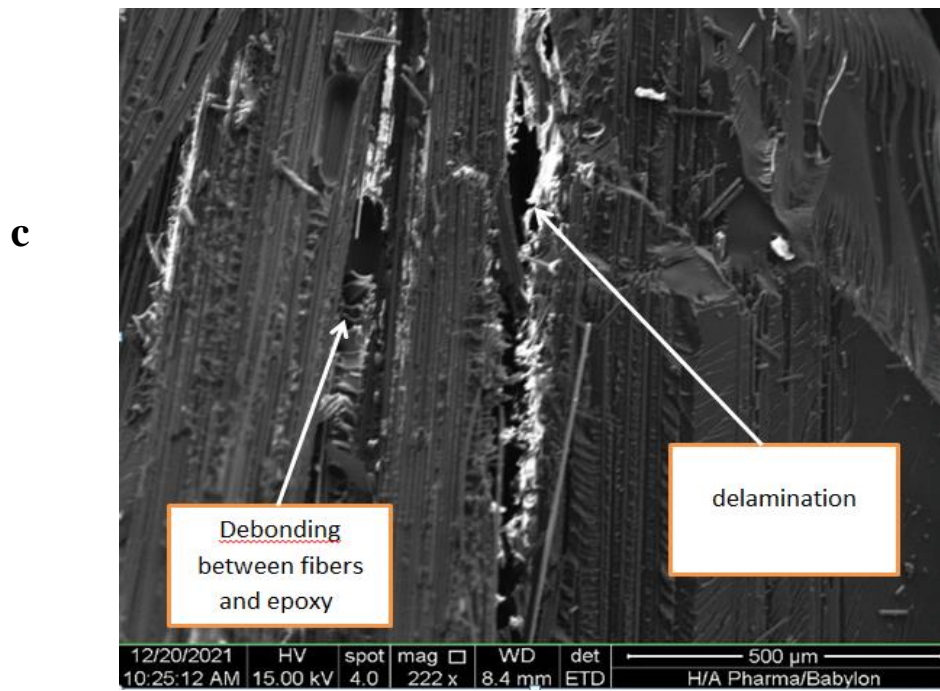
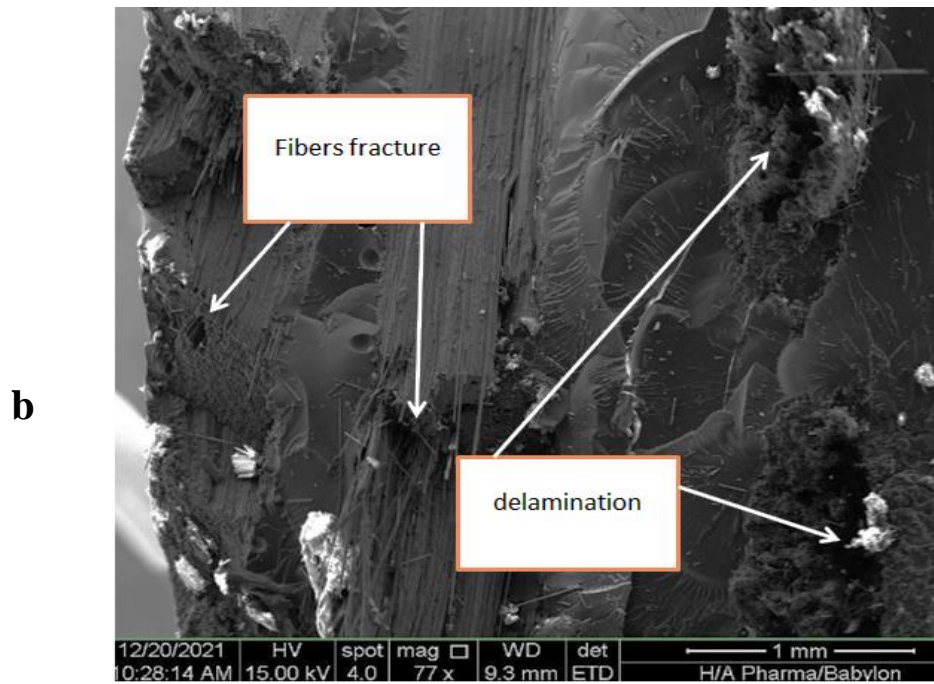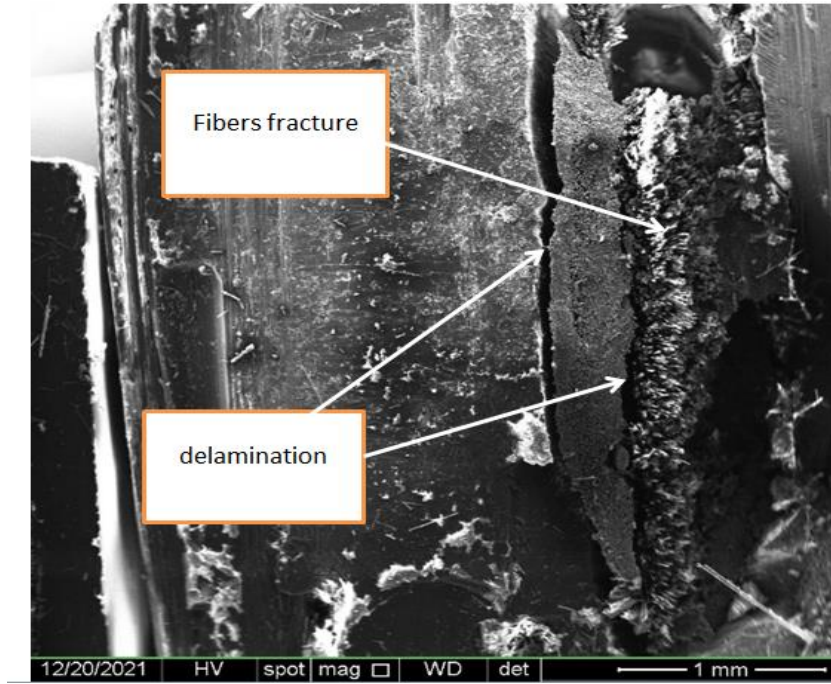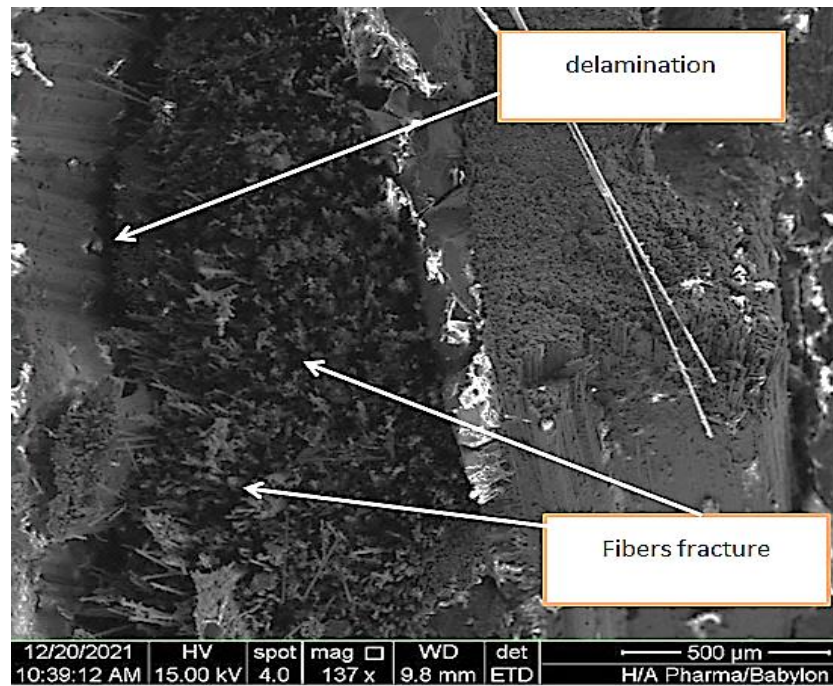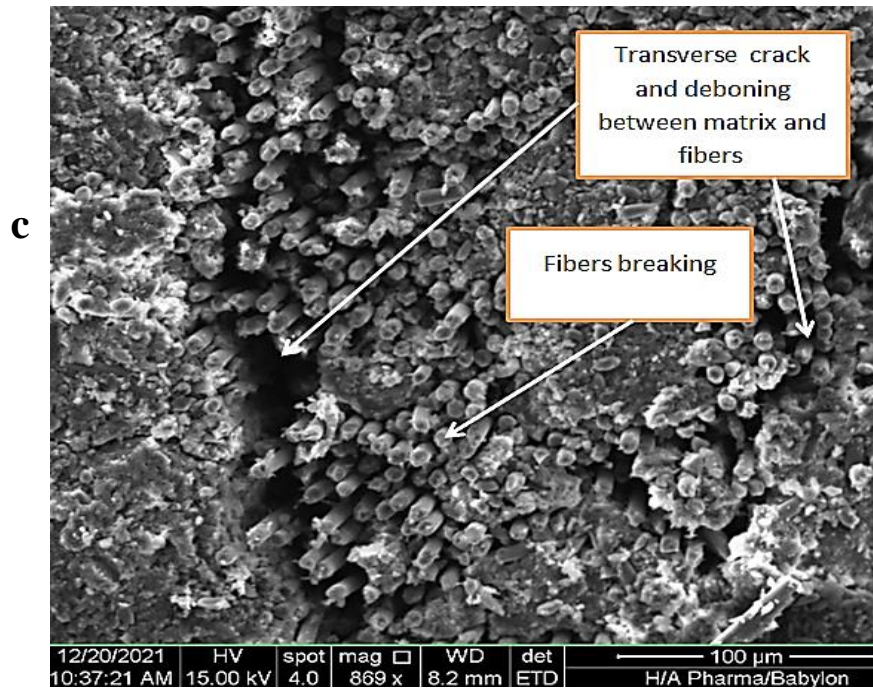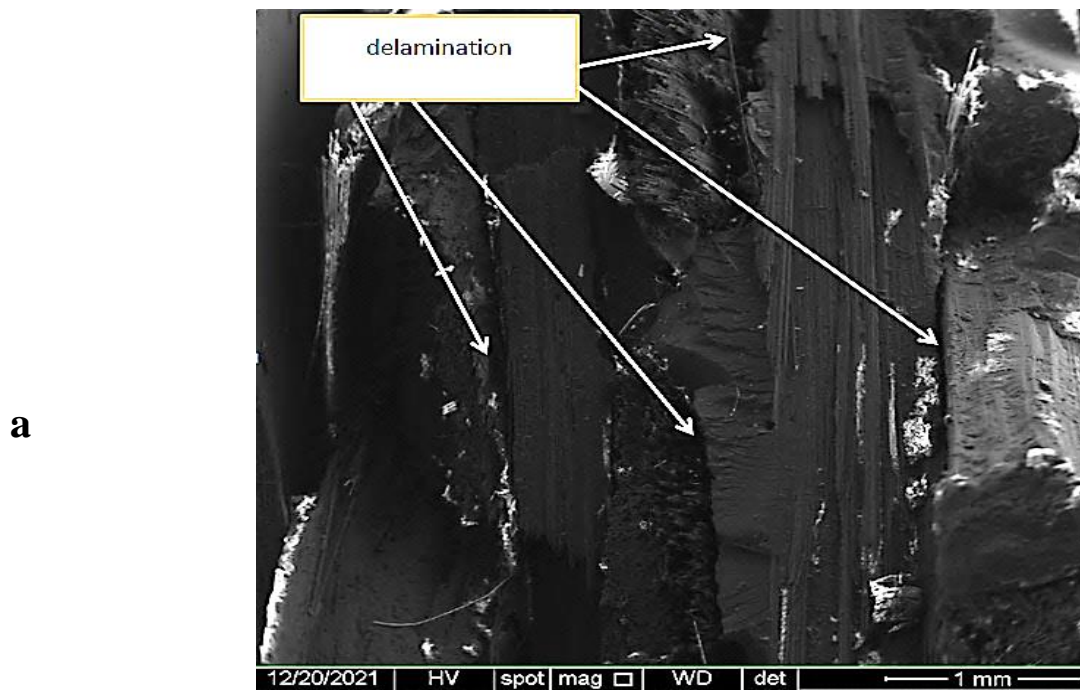Figure 5.11SEM of fatigue failure of laminate [0/30/60/90/75].

Figure 5.12 SEM of fatigue failure of laminate [60/30/0/90/75].

b
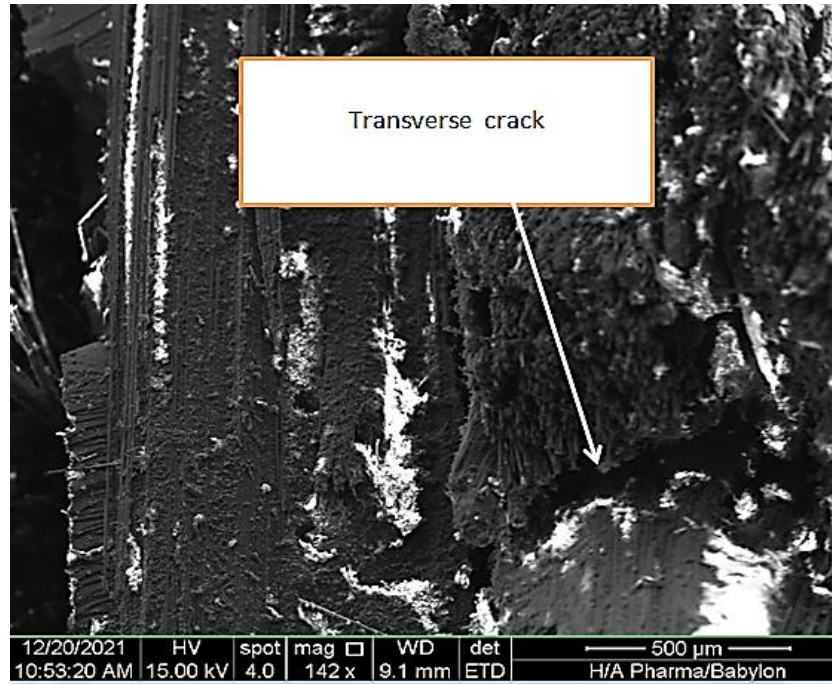
c
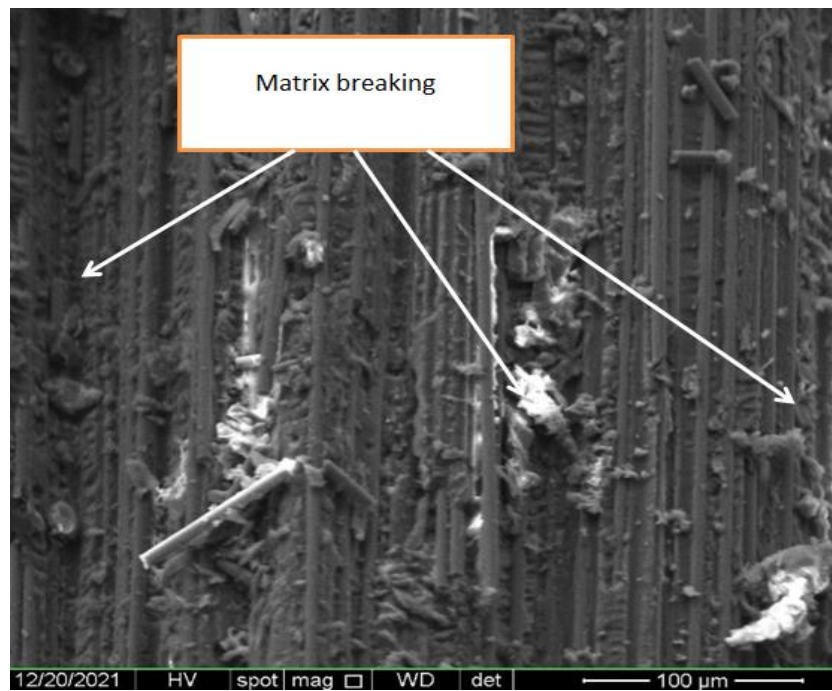
Figure 5.13: SEM of fatigue failure of laminate [30/90/0/60/75].

Chapter six
Conclusions
and
Recommendations

Chapter six

Conclusions and recommendation

6.1 Conclusions

From the experimental and theoretical results obtained, the following main conclusions can be drawn:

1. Failure theories curves converge when the fiber angle increases due to shear between the matrix and the fiber. While, when the fiber angles become more than 45, the strength of lamina become less strength than the epoxy.

2. Hashin's theory gave high acceptance for its use in the unidirectional lamina (carbon/epoxy), followed by Tsai-Hill's theory.

3. There was a convergence between the Maximum stress criterion and the Maximum strain criterion, and the effect of the Poisson ratio was noted in an angles range $(26^{\circ}\text{-}35^{\circ})$. However, they were far from the experimental results.

4. Parameter H_{12} does not affect the theory of Tsai-Wu, as it was neglected.

5. The laminates that start with a ply has an angle of fibers is 0 were the lowest tensile strength, While the laminates that have a layer $(0^{\circ}\text{- orientation fibers})$ in the middle, the tensile strength was high.

6. The theoretical and experimental tensile test results showed that the sequence [60/30/0/90/75] was the best, Where was the different ratio 6.64% .While the different ratio between the theoretical and experimental results of the sequence [0/30/60/90/75] was 27%.

7. The fatigue test of the sequences [60/30/0/90/75],[30/90/0/60/75] and [0/30/60/90/75] was clear, where the laminate with the highest tensile stress got the best fatigue limit.

8. The (SEM) is observed that The breaking of the fibers and the matrix and the removal of interconnection between them was evident, as transverse cracks appeared and delamination of layers. Most of the fractures depended on the angles of the fibers and the effect of the load.

6.2 Recommendation

For future work

1. Study the effect of the volume fraction of laminate CM on its mechanical properties.
2. It is recommended to compare the five theories of the same unidirectional lamina(carbon/epoxy) under the influence of compressive or shear loads.
3. It is recommended to study other theories for comparison with Hashin's theory.
4. Studying the effect of fatigue for different sequences of laminate at different stress ratios(R=0.1,R=0.5).

Reference

Reference

[1]   G. Gupta, A. Kamar, R. Tyagi, and R. Kumar," Application and Future of Composite Materials: A Review", *International Journal of Innovative Research in Science Engineering and Technology (IJIRSET),* vol. 5, pp. 6907- 6911,2016.

[2]   M. K. Sai," Review of Composite Materials and Application", Journal of Latest Trends in Engineering and Technology (IJLTET), vol. 6,pp. 129-135 ,2016.

[3]   D. B.Miracle, "Metal Matrix Composite –From Science to Technology Significance", Composite Science and Technology, vol. 65,pp2526-2540,2005.

[4]   P. D. Pastuszak, and M. Muc, "Application of Composite Materials in Modern Construction", *Key Engineering Materials*, vol. 542, pp 119-129,2013.

[5]   R. M. Florea, and I. carcea, "Polymer Matrix Composite –Routes and Properties", *International Journal of Modern Manufacturing Technologies,* vol. 5,pp 59-64,2012.

[6]   M. Balasubramanian, "Composite Materials and Processing", *Taylor & Francis Group,*2012.

[7]   G. M. N. Islam, B. S. Hassan, A. N. M.A. Haque, M. S. Mukhtar, and S. Shaherbano, " Embryonic Phases of Hard Composites: A Review",*Advance Research in Textile Engineering,* vol. 3,pp 1-8,2018.

[8]   D. K. Rajak, D. B. Pagar, P. l.Menezes, and E. linul," Fiber-Reinforced Polymer Composites: Manufacturing, Properties, and Applications", *MDPI* Journal, vol. 11,pp 1-37,2019.

[9]   D. K.Rajak, D. D. Pagar, R. Kumar, and C I. pruncu," Recent progress of reinforcement materials: a comprehensive overview of composite materials*", Journal of Materials Research and Technology,* vol. 8,pp 6354-6374,2019.

[10]   M. R. Hossain, M. A. Islam, A. V. Vuurea, and I. Verpoest, " Effect of Fiber Orientation on the Tensile Properties of Jute Epoxy Laminated Composite ", *Journal of Scientific Research,* vol. 5, pp. 43-54,2013.

[11]   A. Riccio, G. D. Felice, S. Saputo, and F. Scaramuzzion, "Stacking Sequence Effects on Damage Onset in Composite

Laminate subjected to Low-Velocity Impact", *J. Elsevier,* vol. 88,pp. 222-229,2014.

[12] F. K. Alves de Sousa, I. Ujike, and A. Kadota," Effect of Different Fiber Angles for Composite Material with Fibreglass Reinforced on Mechanical Properties", International Journal of Mining, Metallurgy & Mechanical Engineering (IJMMME), vol. 4,pp 1-6,2016.

[13] M. Koc, F. O. Sonmez, N. Ersoy, and K. Cinar,", Failure Behavior of Composite Laminates Under Four-point Bending", *Journal of Composite Materials,* vol. ,pp. 1-19,2016.

[14] S. Eksi, and K. Genel," Comparison of Mechanical Properties of Unidirectional and Woven Carbon, Glass and Aramid-Reinforced Epoxy Composite", *ACT A Physics Polonnica A,* vol. 132,pp. 879-882,2017.

[15] D. Mohamad, A. Syamsir, S. N. Sa'don, N.M. Zahari, S.A.H.A. Seman, M.F. Razali, and A. Abas," Stacking Sequence Effects on Performance of Composite Laminate Structure Subjected To Multi-Axial Quasi-Static Loading" *IOP Materials Science and Engineering*,2018.

[16] M. Nagamadhu, G. C . Kumar, and A. Jeyaraj," Effect of stacking sequence on mechanical properties neem wood veneer plastic composites", American Institute of Physics -AIP Conference Proceedings,2018.

[17] W. Zhuang, and Wenhong. "An Effect of stacking angles on mechanical properties and damage propagation of plain woven carbon fiber laminates", vol. 5,pp. 1-15,2018.

[18] M. A. Caminero, G. P. Podriguze, J. M. Chacon, and I. G. Morenom, "Tensile and Flexural Damage Response of Symmetric Angle-Ply Carbon Fiber Reinforced Epoxy Laminates: Non-Linear Response and Effects of Thickness and Ply-Stacking Sequence" *Journal Of Applied Polymer Science*, vol 40, pp 3678-3690,2019.

[19] H. F. A. Marzuki, E. A. E. Ubaidillah, S. A. Sivarasa, M. Syamsul, and M. Jaafar," 'Study on Effect of Fiber Orientation on Flexural Properties of Glass Fiber Reinforced Epoxy Composite Laminates for Structure Applications", *Trans Tech Publications*, vol. 301,PP.227-237,2020.

[20]   S. N. Anomani, M. Hunain, and S. H. Aumairee, "Investigation Failure Theory For A lamina of Carbon fiber/epoxy Matrix Composite Materials", *Journal of Engineering Science and Technology,* vol. 15, pp. 846-857,2020.

[21]   A. Choudhury, "First Ply Failure Analysis of Laminated Composite Beam For Different Boundary Condition Under Thermo Mechanical Loading", *Internal Journal of Applied Mechanics And Engineering,* vol. 25,pp. 12-26,2020.

[22]   N. M. Mate, A. A.Kumbhojkar,S. S. Gunjate,A. P. Shrotri,and S. S.Kulkarni, "Study of Effect Orientation of Carbon Fiber on The Strength of Ply Laminates Using Experimental and Finite Element Analysis", *Journal of Information and Computational Science",* vol. 10,pp. 171-177,2020.

[23]   H. L. Kadi, and F. Fllyin, "Effect of Stress Ratio on the Fatigue of Unidirectional glass/epoxy Composite Laminae," *Elsevier Science,*vol.25,pp. 917-924,1994.

[24]   S. Keusch, H. Queck, and K. Gliesche, "Influence of glass fiber/epoxy risen Interface on static mechanical properties of unidirectional composite and on Fatigue Performance of Cross Ply Composite", *Elsevier Science*, vol.29, pp. 701-705,1998.

[25]   E. K. Gamstedt, "Fatigue Damage Mechanism in Unidirectional Carbon Fiber-reinforced plastic", *Journal of Materials Science*, vol.34, pp. 2535-2546,1999.

[26]   X. Diao, L. B. Lessard, and M. M. Shokrieh, "Statistical Model for Multiaxial fatigue behavior of unidirectional plies", Composite Science and Technology, vol. 59, pp. 2025-2035,1999.

[27]   A. R. Bezazi, A. Elmahi, J. M. Berthelot, and B. Bezzazi," Flexural Fatigue Behavior of Cross-Ply Laminates an Experimental Approach", *Strength of Materials*, vol. 35,pp. 149-161,2003.

[28]   M. Kawai, "A phenomenological Model for off-axis Fatigue Behavior of Unidirectional Polymer Matrix Composites under different Stress Ratio", *Elsevier Science*, vol. 35 ,pp. 955-963,2004.

[29]   T. S. Lim, B. C. Kim, and D. G. Lee, "Fatigue Characteristics of the Bolted Joins for Unidirectional Composite Laminates", *Elsevier Science*,vol.72,pp. 58-68,2006.

[30]   F. T. Behrooz, M. M. Shokreih, and L. B. Lessard," Progressive Fatigue Damage Modeling of Cross-Ply Laminates, II: Experimental evaluation", *Journal of Composite Materials,* vol.44, pp.1261-1277,2010.

[31]   M. M. Shokreih, and F. T. Behrooz," Progressive Fatigue Damage Modeling of Cross-Ply Laminates, I: Modelind Strategy", *Journal of Composite Materials,* vol.44, pp.1217-1231,2010.

[32]   H. Katogi, Y. Shimamera, K. Tohgo and T. Fijii, "Fatigue Behavior of Unidirectional Jute Spun Yarn Reinforced PLA", *Advanced Composite Materials,* Vol. 21, pp. 1-10,2012.

[33]   J. Brunbauer, G. Pinter, "Effect of Mean Stress and Fiber Volume Content on the Fatigue –induced Damage Mechanism in CFRP*",* *International Journal of Fatigue,* vol. 75,pp. 28-38,2015.

[34]   A. Hosoi, S. Sakuma, Y. Fujita, and H. Kawada," Prediction of initiation of Transverse crack in cross-ply CFRP Laminates under Fatigue loading by Fatigue properties of Unidirectional CFRP in 90 direction","", *Elsevier Science*, vol.68, pp. 398-405,2015.

[35]   W. Roundi, A. Elmahi, A. Elgharad, and J. L. Rebiere, "Experimental and numerical Investigation of the Effect of Sacking Sequence and Stress Ratio on Fatigue Damage of glass/epoxy Composite", *Elsevier Science*, vol. 109,pp. 64-71,2017.

[36]   M. Nikforooz, J. Montesano, M. Golzar, and M. M. Sholreih, "Fatigue Behavior of Laminated Glass fiber reinforced polyamide ", Procedia Engineering, vol. 213,pp.816-893,2018.

[37]   S. Mandegarian, and F. T. Behrooz, "A general Energy-Based Fatigue Failure Criterion for the Carbon Epoxy Composites", *Composite structures*, vol. 235,pp. 1-33,2020.

[38]   S. D. Bankar, P. N. Kulkarin, V. V. Kulkarni, and N. K. Patil, "Tension-Tension Fatigue Life estimate of CFRP Composite by Model Testing", Journal. Elsevier, vol. 46pp.217-222,2021.

[39]   N. H. Padmaraj, K. M. Vijaya, and P. Dayananda, "Experimental Study on The Tension-Tension Fatigue Behavior of glass/epoxy

Quasi-isotropic Composite*", Journal of Saud University – Engineering Science,* vol. 32,pp. 396-401,2020.

[40]   G. Akovali, "Handbook of Composite Fabrication", First Edition Rapar Technology Limited,2001.

[41]   Y. A. Ergün, "Mechanical Properties of Epoxy Composite Materials Produced with Different Ceramic Powder", *Journal of Materials Science And Chemical Engineering,* vol. 7, pp. 1-8,2019.

[42]   P. Theori, P. Sharama, and M. Bhargava, "An Approach Composite Materials in Industrial Machinery: Advantages, Disadvantages, and Applications", *International Journal of research in Engineering andTechnology(IJRET),*vol. 2,pp. 350-355,2013.

[43]   S. Chand, "Review Carbon fiber of Composite", *Journal of Materials Science,* vol. 35,pp. 1303-1313,2000.

[44]   D. F. Adams, L. A. Carlsson, and R. B. Pipes, "Experimental Characterization of Advanced Composite Materials", Third Edition CRC Press,2003.

[45]   G. Yerbolat, M. H. Ali, N. Badanova, A. Ashirbeob, and G. Islam "Composite Materials properly Determination by Rule of Matrix Monte Carlo Simulation", *International Conference on Advanced Manufacturing*, vol. 5,pp.78-80,2018.

[46]   V. V. Vasiliev, and E. V. Morozo, "*Advanced Mechanics of Composite Materials",* First edition, *Elsevier's Science & Technology,*2007.

[47]   C. Decolon, "Analysis of Composite Structures", Hermes Penton Ltd,2002.

[48]   M. K. Buragohain, *Composite structures: design, mechanics, analysis, manufacturing, and testing*. CRC Press, 2017.

[49]   I. M. Daniel, and O. Ishai," *Engineering Mechanics of Composite Materials*", Second edition, Oxford University Press,2006.

[50]   R. M. Jones, *Mechanics of composite materials*. Second Edition, Taylor and Francis CRC Press, 1999.

[51]   M. Rajanish, N. V. Nanjundaradhya, R. S. Sharma, and B. Pal*, "*A review of Failure of Composite Materials*", Journal of Engineering Research and Applications"*, vol. 3,pp. 122-124,2013.
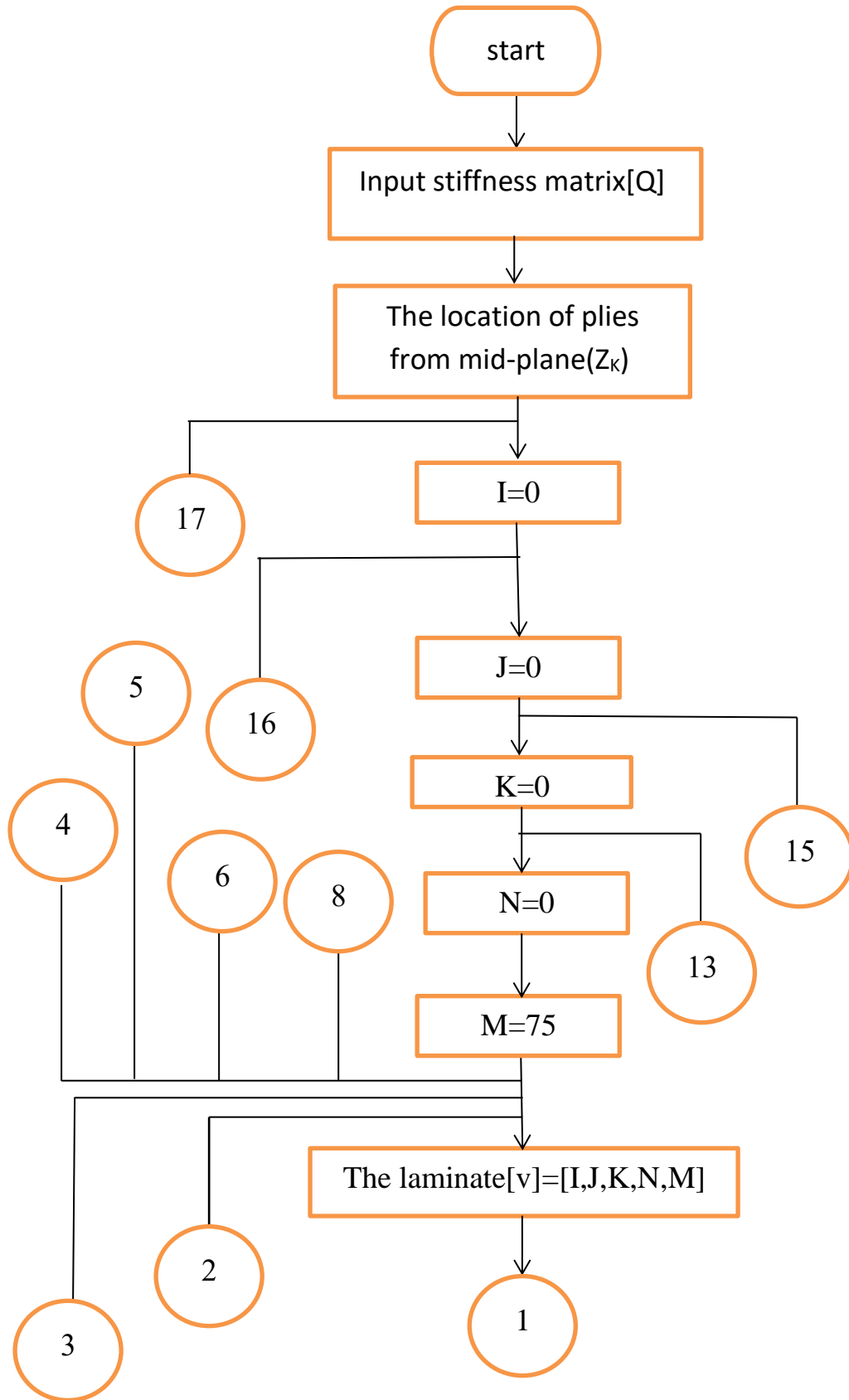
[52]   I. M. Daniel, "Failure of Composite Materials Under Multi-axial Static and Dynamic Loading", Procedia Engineering, vol.88, pp 10-17,2014.

[53]   S. Li," The Maximum Stress Failure Criterion and the Maximum Strain Failure Criterion: Their Unification and Rationalization", *Journal of Composite Science",* vol. 4, pp.2020.

[54]   A. K. Kaw, "Mechanical of Composite Materials", second edition, Taylor and Francis Group, CRC Press, 2006.

[55]   Y. G. Qing, R. Yi-Ru, Z. Tian-tian, X. Wan-Shen, and J. Hong-Yong, "Hashin Failure Theory-Based Damage Assessment Methodology of Composite Tidal Turbine Blade and Implications for the Blade Design", *China Ocean Eng,* vol. 32,pp. 216-225,2018.

[56]   M. J. Suriani, A. Ali, S. M. Sapuan,and A. Khalina,"Aspect of Fatigue Analysis of Composite Materials :A review", Pertanika J. Sci. &Technol, Vol. 21,pp. 1-14,2013.

[57]   J. Degrieck, and W. V. Paepegem, "Fatigue Damage Modeling of Fiber-reinforced Composite Materials: A review", Appl. Mech. Rev, vol. 54,pp.279-300,2001.

[58]   T. Jeannin, X. Gbarion, E. Ramasson,and Placet,"A bout the Fatigue Endurance of Unidirectional Flax-epoxy Composite Laminates", *Composite Part B: Engineering*, vol. 165,pp. 690-701,2019.

[59]   T. Properties ,S,Quikmast, I.M. Packer, andT.D.sheet,"Quikmast 105",1985.htt://dcp-int.com/iq/index.php?p=about.

[60]   Product Datasheet, https://che.sika.com, Edition 26.09.2012, Version no. 3. Pdf.

[61]   Standard Test Method for Tensile Properties of Plastics, ASMD638-14,http://www.astm.org/standards/D638.htm.

[62]   ASTM D3039 / D3039M-17, Standard Test Method for Tensile Properties of Polymer Matrix Composite Materials, ASTM International, West Conshohocken, PA, 2017, www.astm.org.

[63]   A. N. Al-khazraji, and M. N. Shareef, "Comparison of Fatigue Life Behavior Between Two Composite Materials Subjected to Shot Peening at Different Time", *Al-Khwarizmi Engineering Journal*, vol.10, pp. 1-12,2014.

[64]   J. Petermann, A. Plumtree, "A unified Fatigue Failure Criterion for Unidirectional Laminates", *Composite Part B: Engineering*, vol. 32,pp. 107-118,2001.

[65]   Jaafar. M. Akhudair," Study of fatigue and tribological properties of hybrid composite Materials", Master's Thesis, University of Babylon, Iraq,2021.

Appendices

Appendix

Appendix (A): The flowchart for MATLAB program.

start

Input stiffness matrix[Q]

The location of plies from mid-plane(Z_K)

I=0

17

J=0

5

16

4

K=0

6

8

N=0

15

13

M=75

The laminate[v]=[I,J,K,N,M]

2

3

1

A-1

1

2 Yes

3

I≠J

No

Yes

I≠K

No

4

Yes

I≠N

5

No

Yes

J≠K

6

Yes

No

J≠N

No

7

```
        ┌────┐
        │ 11 │
        └────┘
           │
           ▼
┌─────────────────────────────────────┐
│  The global stain as equation (3.72) │
└─────────────────────────────────────┘
           │
           ▼
┌──────────────────────────────────────┐
│  The global stress as equation (3.73) │
└──────────────────────────────────────┘
           │
           ▼
┌─────────────────────────────┐
│   transformation matrix as  │
│       equation (3.61)       │
└─────────────────────────────┘
           │
           ▼
┌─────────────────────────────┐
│  The local stress as equation│
│            (3.59)           │
└─────────────────────────────┘
           │
           ▼
┌─────────────────────────────────┐
│  Stress ratio for 5 layers according│
│    of  mode failure theories    │
└─────────────────────────────────┘
           │
           ▼
┌─────────────────────────────┐
│  Tensile stress=stress ratio │
│          /thickness         │
└─────────────────────────────┘
           │
           ▼
        ┌────┐
        │ 12 │
        └────┘
```
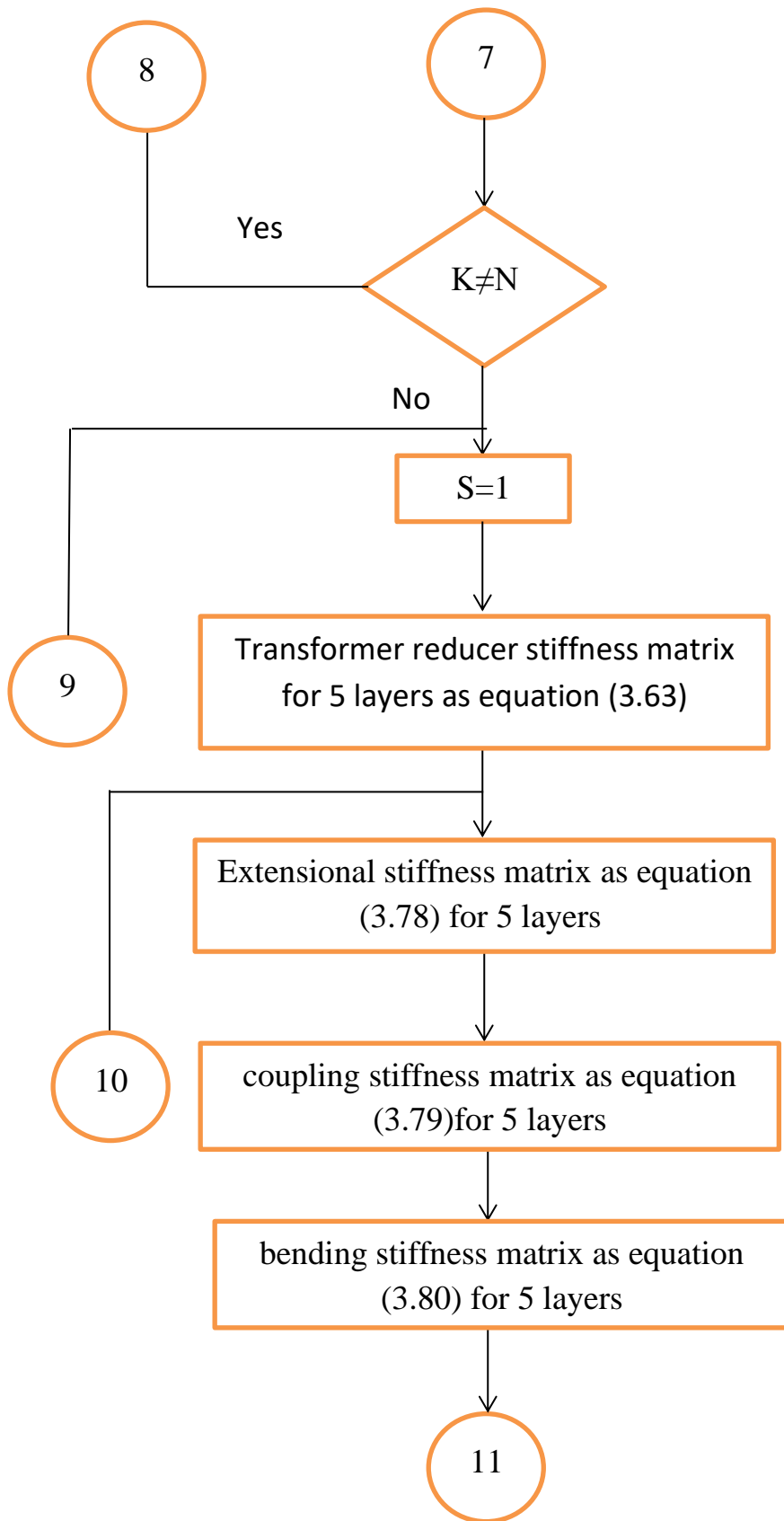
10

Transformer reducer stiffness matrix for this layer equal zero

12

If the strength ratio of any layer is equal the lowest strength ratio (R=R_{PLY})

yes

9

S=S+1

yes

S<5

No

No

13

Print the maximum stress

N=N+30

yes

N<90
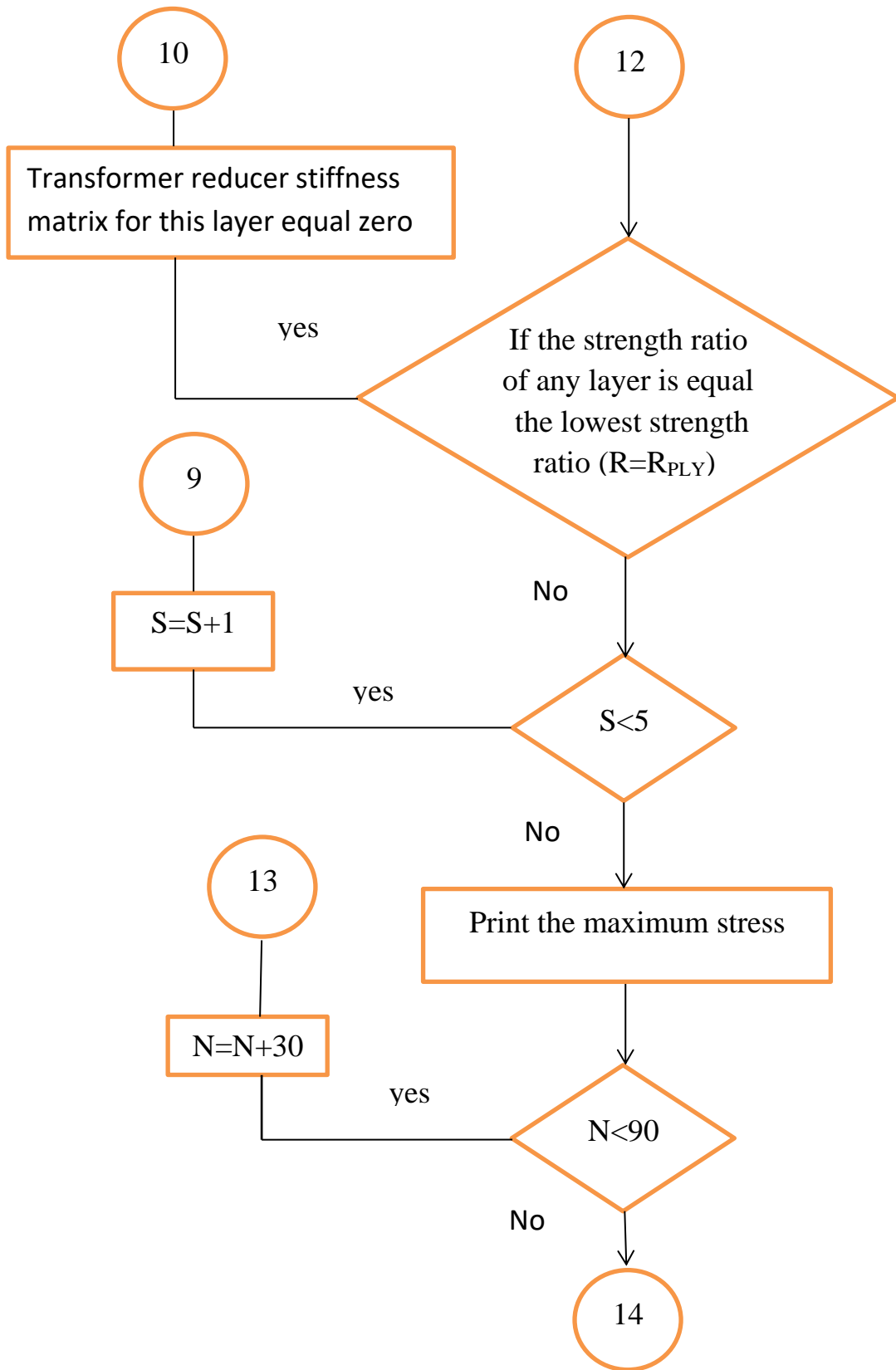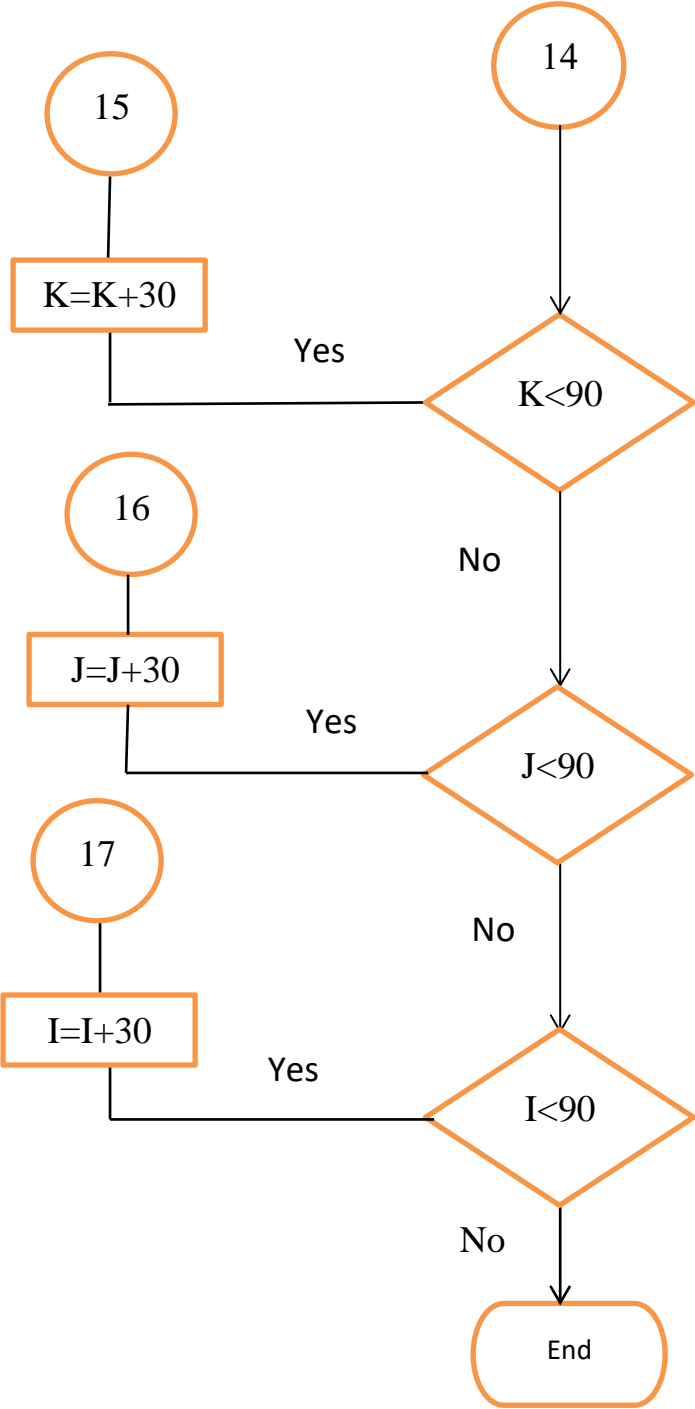
No

14

الخلاصة

في هذا البحث. سيتم دراسة تأثير اتجاه الألياف وتنضيد الرقائق على الخواص الميكانيكية (القوة والصلابة والكلال) للمادة المركبة (الكربون / الايبوكسي). حيث تم تصنيع صفائح المواد المركبة باستخدام تقنية القولبة اليدوية مع التفريغ بنسبة حجمية 30% . يتضمن هذا البحث اختيار نظرية الفشل المناسبة من خلال مقارنة نتائج اختبار الشد العملي للرقائق المركبة احادية الاتجاه المصنوعة من الكربون والايبوكسي بتوجهات الياف مختلفة($0°$ الى $90°$) مع نظريات الفشل الخمسة (نظرية الإجهاد الأقصى ، ونظرية الانفعال الأقصى ، ونظرية تساي - هيل ، ونظرية تساي - وو ، ونظرية هاشين). وتقديم دراسة نظرية حول تاثير تنضيد الرقائق بزوايا مختلفة ($90°$,$75°$,$60°$,$30°$,$0°$) على قوة الشد باستخدام نظرية هاشين ، قوانين المرونة للمواد المركبة ، و نظرية التصفيح التقليدية للحصول على أفضل تنضيد باستخدام برنامج الماتلاب. تم إجراء اختبار الشد لثلاثة من التنضيدات ، حيث يمثل التنضيد [75/90/0/30/60] أعلى قيمة شد ، ويمثل التنضيد [75/60/0/90/30] قيمة الشد الوسطى ، و التنضيد [75/90/60/30/0] يمثل أدنى قيمة للشد. كانت نسبة الفرق بين نتائج قيمة الشد النظرية والتجريبية للتنضيد [75/90/0/30/60] هي 6.64%. بينما كانت نسبة الفرق بين نتائج قيمة الشد النظرية والتجريبية للتنضيد [0/90/30. / 75/60] هي 9.39%. أما بالنسبة للتنضيد [75/90/60/30/0] فكانت النسبة المئوية للفرق 27%.تم الحصول على خصائص الكلال لثلاثة تنضيدات من الصفائح الطبقية ذات الرقائق المائلة ، والمذكورة أعلاه تم قياسها تجريبياً تحت نسبة إجهاد ثابتة 1- = R بحمل ثني معكوس بالكامل. أظهرت النتائج أن التنضيد [75/90/0/30/60] الذي يحتوي على أعلى مقاومة للشد كان له حدود كلال أفضل حيث عدد الدورات كانت اكبر من 10^6 ومقاومة الكلال 60.08 ميكاباسكال.تم استخدام المجهر الالكتروني الماسح لفحص البنية المجهرية للعينات الفاشلة للتنضيدات أعلاه نتيجة اختبار الكلال مثل كسر الالياف وكسر المصفوفة ، وإزالة الترابط بين المصفوفة والألياف ، والتفكيك ، وظهور الشق العرضي، وأن شكل الفشل كان متشابهًا إلى حد ما في جميع التسلسلات ، لكنه اختلف في بداية الضرر من رقيقة إلى أخرى بسبب موقع تلك الرقيقة في الطبقة وابتعادها من مركز التحميل.

دراســـة الخواص الميكانيكية للمادة المركبة المقواة بواسطة الياف احادية الاتجاه

رســــالة مقدمـــة الـــى

جامـــعة كـــــربلاء كلـــية الهنــــــدسة

كجزء مـن متطلـــبات نيـل شهــادة المـاجسـتير

في عــلـوم الهنــدســـة الميكـــانيكية(الميكانيك التطبيقي)

اعدت من قبل

ميثم عبد العباس عليوي

(بكالوريوس 2001)

اشراف

أ.م. د. مصطفى باقر الخفاجي	أ.م .د. صلاح نوري النعماني

2022 AD	1443 هـ